Journal of Medicinal Chemistry

Article

Design and synthesis of N-aryl-phthalimides as inhibitors of glucocorticoid- induced TNF receptor-related protein, pro-inflammatory mediators, and cytokines in carrageenan-induced lung inflammation

Mashooq Ahmad Bhat, Mohamed A Al-Omar, Mushtaq A Ansari, Khayry M Zuheir, Faisal Imam, Sabry M Attia, Saleh A Al-Bakheet, Ahmed Nadeem, Hesham Korashy, Andrew Voronkov, Vladimir Berishvili, and Sheikh Ahmad

J. Med. Chem., **Just Accepted Manuscript** • DOI: 10.1021/acs.jmedchem.5b00934 • Publication Date (Web): 10 Oct 2015

Just Accepted

ACS Publications

Journal of Medicinal Chemistry is published by the American Chemical Society. 1155 Sixteenth Street N.W., Washington, DC 20036

Graphical Abstract

Design and synthesis of *N*-aryl-phthalimides as inhibitors of glucocorticoid-induced TNF receptor-related protein, pro-inflammatory mediators and cytokines in carrageenan-induced lung inflammation

Mashooq A. Bhat*, Mohamed A. Al-Omar, Mushtaq A. Ansari, Khairy M. A. Zoheir, Faisal Imam, Sabry M. Attia, Saleh A. Bakheet, Ahmed Nadeem, Hesham M. Korashy, Andrey Voronkov, Vladimir Berishvili, Sheikh F. Ahmad*

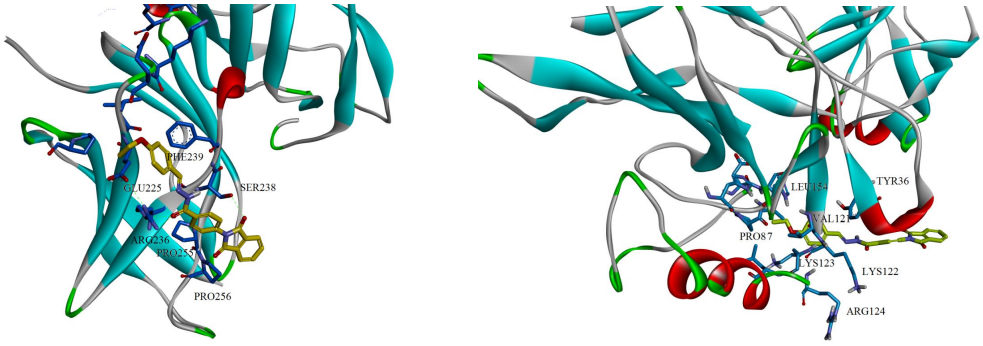

Design and synthesis of *N*-aryl-phthalimides as inhibitors of glucocorticoid-induced TNF receptor-related protein, pro-inflammatory mediators and cytokines in carrageenan-induced lung inflammation

Mashooq A. Bhat[a,♯,*], Mohamed A. Al-Omar[a], Mushtaq A. Ansari[b], Khairy M. A. Zoheir[b], Faisal Imam[b], Sabry M. Attia[b], Saleh A. Bakheet[b], Ahmed Nadeem[b], Hesham M. Korashy[b], Andrey Voronkov[c,d,e], Vladimir Berishvili[c], Sheikh F. Ahmad[b,♯,*]

[a]*Department of Pharmaceutical Chemistry, College of Pharmacy, King Saud University, Riyadh Kingdom of Saudi Arabia*

[b]*Department of Pharmacology and Toxicology, College of Pharmacy, King Saud University, Riyadh, Kingdom of Saudi Arabia*

[c]*Department of Chemistry, Lomonosov Moscow State University, Leninskie Gory, 1/3, Moscow 119991, Russia*

[d]*Digital BioPharm ltd., 145-157 St. John Street, London, UKEC1V 4PW*

[e]*Moscow Institute of Physics and Technology (State University), 9 Institutskiy Lane, Dolgoprudny City, Moscow Region 141700, Russia*

Author information

[*]Corresponding authors

[*]M. A. Bhat: Phone +966-558164097; E-mail: mabhat@ksu.edu.sa

[*]S. F. Ahmad: +966-569496770; E-mail: fashaikh@ksu.edu.sa

Author contributions

[♯]M. A. Bhat and S. F. Ahmad contributed equally to this work.

Abstract

N-aryl phthalimides **(1-10P)** derived from thalidomide by insertion of hydrophobic groups were evaluated for anti-inflammatory activity and compound (4-(1,3-dioxo-1,3-dihydro-2*H*-isoindol-2-yl)-*N*'-[(4-ethoxyphenyl)methylidene]benzohydrazide **6P** was identified as a promising anti-inflammatory agent. Further testing confirmed that compared with the control, **6P** treatment resulted in a considerable decrease in $CD4^+$, NF-κB $p65^+$, TNF-α^+, IL-6^+, $GITR^+$ and IL-17^+ cell populations and an increase in the $Foxp3^+$, $CD4^+Foxp3^+$ and IκBα^+ populations in whole blood and pleural fluid of a mouse model of lung inflammation. Moreover, treatment with the compound **6P** decreased the proteins associated with inflammation including TNF-α, IL-6, IL-17, GITR, NF-κB, COX-2, STAT-3, and iNOS and increased the anti-inflammatory mediators such as IL-10 and IL-4. Further, histopathological examination confirmed the potent anti-inflammatory effects of the compound **6P**. Thus, the *N*-aryl phthalimide derivative **6P** acts as a potent anti-inflammatory agent in the carrageenan-induced lung inflammation model suggesting that this compound may be useful for the treatment of inflammation in a clinical setting.

Keywords: Phthalimide derivatives, Anti-inflammatory activity, Carrageenan induced lung inflammation; inflammatory mediators; Pleural exudate; Lung tissue.

1. Introduction

Thalidomide (α-*N*-phthalimido glutarimide) and its derivatives are known to have immunomodulatory and anti-inflammatory activities and represent potential preventive therapies for autoimmune diseases. Initially introduced in 1954 as a sedative, thalidomide was later withdrawn from the market due to its teratogenic effects. Nevertheless, thalidomide possesses various pharmacological properties and has since been approved and used successfully for treatment of inflammatory and autoimmune diseases[1] including erythema nodosum leprosum and multiple myeloma.[2] Thalidomide or its analogs have shown their effect in the treatment of rheumatoid arthritis, Crohn's disease, prostate cancer, Behcet's disease, chronic host-versus-graft disease, lupus erythematosus, and HIV-associated oral ulcers.[3-5] In addition, previous studies have confirmed that thalidomide exerts its anti-inflammatory effects by suppressing the production of pro-inflammatory molecules including TNF-α, IL-1β, IL-6, and NO.[6-7] The benefits of thalidomide administration in patients include relief of peripheral pain and inflammation, which have been confirmed in several animal models as well.[8-9] However, the teratogenicity, peripheral neuropathy, and other adverse effects of thalidomide have prompted the design of novel analogs that exhibit low toxicity and enhanced potency in blocking cytokine production.[10] Still, few groups have investigated structural modification of thalidomide as a means to obtain potent inhibitors of TNF-α and inflammation. Replacement of the glutarimide moiety of thalidomide with a methyl (3,4-dimethoxyphenyl) propionate or 2,6-diisopropylphenyl moiety, having fluorine or amino substitution in the homocycle of thalidomide, have produced analogs with enhanced tumor necrosis factor inhibitor activity.[11-12]

This manuscript describes the design, synthesis, and evaluation of the anti-inflammatory effects of *N*-arylphthalimide derivatives **(1-10P)**. The rationale underlying the design of new

derivatives **(1-10P)** was to obtain more lipophilic phthalimide derivatives with potent anti-inflammatory activities. To this end, *N*-arylphthalimide derivatives, which are based on a thalidomide structural analogue (LASSBio 595), were attained by modulating the thiomorpholine moiety with hydrophobic groups in order to increase the lipophilicity of the targeted compounds (Figure 1).

Carrageenan (Cg)-induced pleurisy is a well-established model of acute inflammation characterized by a rapid influx of polymorphonuclear leukocytes (PMLs) followed by mononuclear cell infiltration into the lungs.[13-14] The onset of Cg-induced acute inflammation has been linked to neutrophil infiltration and the production of neutrophil-derived free radicals such as hydrogen peroxide, superoxide, and hydroxyl radicals.[15] Moreover, this model is often used to assess the anti-inflammatory effects of pharmaceutical agents and the *in vivo* importance of established inflammatory mediators.[16-17]

In the present study, we hypothesized that *N*-arylphthalimide derivatives **(1-10P)** may affect Cg-induced lung inflammation due to anti-inflammatory and immunosuppressive activities of phthalimide pharmacophore. Consequently, we decided to investigate whether treatment with *N*-arylphthalimide derivatives could prevent the development of Cg-induced lung inflammation in mice. Thus, we first investigated the effects of compounds **(1-10P)** on the malondialdehyde (MDA) levels, and myeloperoxidase (MPO) and glutathione (GSH) activities, as these are all markers of the inflammatory process. Further, more detailed studies were carried out on one of the active compounds (**6P).** The presence of $CD4^+$, NF-κB $p65^+$, TNF-α^+, IL-6^+, $GITR^+$, IL-17^+, Forkhead box $P3^+$ ($Foxp3^+$), $CD4^+Foxp3^+$, and IκBα^+ expressing cells in pleural exudates and in heparinized blood were assessed using flow cytometry. Moreover, the levels of cytokines produced by Th1 and Th2 cells were analyzed using enzyme-linked immunosorbent assay (ELISA) of

pleural fluid following intrapleural Cg administration. We also evaluated TNF-α, IL-17, NF-κB, COX-2, STAT-3, iNOS, and IL-10 mRNA expression in lung tissue using RT-PCR, and GITR, COX-2, STAT-3, NF-κB p65, and IκBα protein expression in lung tissues using western blotting. Histopathological examination of lung tissues was also performed.

2. Results and discussion

2.1. Chemistry. 4-Amino benzoic acid hydrazide **(1)** was prepared by the reaction of 4-aminobenzoate (benzocaine) with hydrazine hydrate in absolute ethanol**.** 4-Amino-*N*'-[substituted phenylmethylidene]benzohydrazide **(2a-j)** were synthesized by the condensation of **1** with different substituted benzaldehydes in the presence of ethanol and a few drops of glacial acetic acid.[18] The resulting 4-Amino-*N*'-[substituted phenylmethylidene]benzohydrazide **(2a-j)** were chosen as starting compounds to design several *N*-arylphthalimide derivatives **(1-10P)**. Target compounds, 4-(1,3-dioxo-1,3-dihydro-2*H*-isoindol-2-yl)-*N*'-[substituted phenylmethylidene]benzohydrazide **(1-10P),** were synthesized by the reaction of 4-amino-*N*'-[substituted phenylmethylidene]benzohydrazide **(2a-j)** with phthalic anhydride in glacial acetic acid with yields between 58-80% (Scheme 1).[19] The final compounds were characterized by FT IR, ^{1}H NMR, ^{13}C NMR, and mass spectroscopy. The IR spectrum revealed bands for CONH, N=CH, C=O groups at 3459-3258, 3065-2836 and 1740-1686 cm^{-1}, respectively. The ^{1}H NMR spectra of **(1-10P)** confirms the presence of Ar-H, CONH, and N=CH protons by showing signals at δ: 7.0-8.5, 11.4-12.2 and 8.3-10.8 ppm, respectively.[20] Also, the ^{13}C NMR of the compounds **(1-10P)** were found to be in agreement with their chemical structures. Additionally, all the compounds gave corresponding molecular ion peaks in mass spectra as determined by the triple quadrupole LC/MS.

2.2. Effect on general behavior and acute toxicity in mice. Compound **6P** was administered by oral gavage in a single dose of 2000 mg/kg. The animals were observed for any toxic symptoms and death over a period of 7 days. The animals tolerated this dose without any toxic symptoms. The animals became sluggish after treatment but recovered within 2 h of the treatment, which confirmed the absorption of the test compound. We did not observe any signs of toxicity or death during this period. These results indicate that compound **6P** exhibits no toxicity and is well tolerated by experimental animals at the tested dose.

2.3.Effect of compounds (1-10P) on biochemical analysis. Our preliminary study investigated the effect of compounds **(1-10P)** on oxidative parameters during the acute phase of inflammation. We measured the level of malondialdehyde (MDA) in lung tissue from normal control (NC) mice, carrageenan (Cg)-injected mice, and Cg-injected mice pre-treated with compounds **(1-10P)** at 10, 20 and 40 mg/kg, i.p. As shown in Table 1, injection of mice with Cg resulted in an increase in MDA as compared to mice in the NC group. In contrast, pre-treatment of Cg-injected mice with compounds (1, 3-7, 9, and 10P) resulted in a significant reduction in lung MDA, with the most significant effect observed for compound **6P** at 20 and 40 mg/kg $P<0.01$). Moreover, a minimum significant ($P<0.05$) reduction in MDA was also observed at 10 mg/kg. MDA, a lipid peroxidation biomarker, leads to activation and formation of free radicals by pulmonary endothelial cells and neutrophils, increased production of adhesion molecules, and generation of cytokines and chemokines that elicit the recruitment of macrophages and neutrophils within the pulmonary microvasculature.[21]

Carrageenan-injected animals exhibited a substantial increase in lung tissue MPO, which is believed to indicate PML infiltration and lipid peroxidation.[22] Tissue MPO activity is a sensitive and specific marker for acute inflammation and reflects polymorphonuclear cell infiltration of the

parenchyma. Thus, we further examined the effect of compounds **(1-10P)** on MPO activity in the lung tissue. The results illustrate that the MPO activity was markedly increased in the Cg group. Importantly, treatment of mice with compounds **(1-7, 9, and 10P)** prior to injection with Cg resulted in a reduction in the MPO activity. Further, the results show that compound **6P** is the most potent at reducing the activity of MPO. Therefore, these results indicate that compound **6P** exhibits marked anti-inflammatory activity.

In addition, Cg-injected mice showed reduced GSH activity as compared to untreated mice, an effect that was reversed in mice treated with compounds **(1, 3, 6-10P)**. Consistent with our initial findings, the most significant increase in GSH activity was found in mice treated with compound **6P**. GSH has pleiotropic roles including the maintenance of cells in a reduced state, serving as an electron donor for certain anti-oxidative enzymes and in the formation of conjugates with some harmful endogenous and xenobiotic compounds *via* catalysis of glutathione s-transferase;[23] thus, the ameliorating effects of compound **6P** on GSH demonstrated a further beneficial effect of its administration. Together, our preliminary studies demonstrate that compound **6P** significantly decreases the level of MDA and MPO activity and increases GSH activity *in vivo*. These findings indicate that *in vivo* anti-inflammatory activities of compound **6P** attenuate the degree of acute inflammation in this model system.

2.4. Effect of compound 6P on $CD4^+$, $Foxp3^+$, and $CD4^+Foxp3^+$ cells in whole blood.

T cells expressing the transcription factor Foxp3 are known to play a key role in the immune system apparatus that controls regulatory T cell (Treg) development, function, and inflammatory processes.[24] Furthermore, a recent study suggested that Foxp3 expression in lung epithelial cells suppresses inflammation *via* inhibition of chemokine secretion.[25] Therefore, we assessed the effect of compound **6P** on the composition of responding T cell populations using flow cytometry. There

was a substantial increase in the percentage of $CD4^+$ cells in the Cg group compared with the NC group, an effect that was reversed by treatment with compound **6P**. The results revealed that the Cg group exhibited a significant decrease on the percentage of $Foxp3^+$ and $CD4^+Foxp3^+$ cells compared to the NC group. Importantly, following treatment of mice with compound **6P** there was a marked increase in the proportion of $Foxp3^+$ and $CD4^+Foxp3^+$ expressing cells as compared to mice treated with Cg alone (Figure 2A). These results suggest that the anti-inflammatory action of compound **6P** in the mouse model of pleurisy can be, in part, attributed to the reduction of $CD4^+$ cells concomitant with an increase in $Foxp3^+$ T cells at the site of lung inflammation.

2.5. Effect of compound 6P on NF-κB p65$^+$ and IκBα$^+$ cells in whole blood. NF-κB is a transcription factor known to be a major player in regulating the expression of pro-inflammatory mediators that participate in the inflammatory response.[26] Inappropriate regulation of NF-κB is directly involved in a wide range of human disorders including inflammatory bowel disease and numerous other inflammatory conditions. Thus, agents that inhibit NF-κB activation have anti-inflammatory effects.[27] Therefore, we studied the effect of compound **6P** on the percentage of cells expressing NF-κB p65 and IκBα. As shown in Figure 3A, the proportion of NF-κB p65 positive cells increased in the Cg group over that seen in the NC group, an effect that was ameliorated following treatment with compound **6P**. Moreover, as expected, the inverse effect was seen in regard to IκBα$^+$ cells. Together, these results suggest that the anti-inflammatory actions of compound **6P** in the mouse model of pleurisy can be attributed to a reduction in NF-κB activation and corresponding increase in IκBα$^+$ cells at the site of inflammation.

2.6. Effects of compound 6P on the release of carrageenan-induced pro-inflammatory cytokines in pleural exudates. Thalidomide has been shown to selectively inhibit TNF-α production by human monocytes.[28] The ability of thalidomide to inhibit IL-6 and TNF-α production has been

associated with its clinical benefits in the treatment of many inflammatory immune diseases.[29] Moreover, TNF-α and IL-6 play key roles in the induction and perpetuation of inflammation by activating macrophages and upregulating other pro-inflammatory cytokines and endothelial adhesion molecules,[30] and suppressing these pro-inflammatory cytokines have been found to reduce the severity of the inflammatory reaction.[31] Thus, we assessed the effects of compound **6P** on TNF-α and IL-6 production. Administration of Cg alone resulted in a significant increase in TNF-α and IL-6 production in the pleural exudate as compared to the NC group. Furthermore, treatment of mice with compound **6P** caused a significant decrease in the number of TNF-α^+ and IL-6^+ positive cells (Figure 4A). The results of our study highlight the complex network of cytokines that contribute to the initiation and maintenance of inflammation. Furthermore, the ability of compound **6P** to suppress TNF-α and IL-6 production may be one of the factors underlying the anti-inflammatory effects of **6P** on Cg-induced lung inflammation. Administration of Cg alone or before 4-MeH (to induce pleurisy) resulted in a significant decrease in TGF-β1 and IL-10 levels compared to the control group

2.7. Compound 6P reduces the proportion of cells in pleural exudates expressing GITR and IL-17. It is well known that GITR plays a co-accessory role in effector T cell activation, which is further potentiated by the inhibition of Treg cell function, and triggering of GITR on effector CD4 T lymphocytes plays a role in the development of chronic inflammation.[32] Moreover, a recent study provides evidence that mice lacking GITR ($GITR^{-/-}$) have decreased development of lung injury, decreased PML infiltration into the lung, lower levels of TNF-α, IL-1β, and stress oxidative products, and decreased activation of NF-κB.[33] The suppression of pro-inflammatory cytokines has been found to reduce the severity of the inflammatory reaction, and IL-17 is known to be a critical mediator of neutrophil recruitment and migration.[34] Therefore, we assessed the

effect of compound **6P** on the total percentage of $GITR^+$ and $IL\text{-}17^+$ cells during the Cg-induced inflammatory process. As illustrated, the significant finding of the up regulation of GITR expression in the Cg group was more significant as compared with the NC group. Further, we found that compound **6P** significantly reduced the total percentage of $GITR^+$ and $IL\text{-}17^+$ cells (Figure 5A). These findings further suggest that the anti-inflammatory effects of compound **6P** are due to the downregulation of the production and/or secretion of pro-inflammatory cytokines.

2.8. Effect of compound 6P on Th1 and Th2 cytokine levels in serum. The formation of pro-inflammatory cytokines including IL-2 and IL-6 are central to the pathophysiology of inflammation. Overexpression of the pro-inflammatory cytokine IL-2, which is crucial for the maintenance of immune homeostasis and exhibits proinflammatory activities, is well documented in a number of inflammatory processes.[35,36] IL-2 also stimulates the production of TNF-α, IFN-γ, and granulocyte macrophage colony-stimulating factor (GM-CSF).[37] In addition, IL-6 plays a complex role in inflammation, as it can both promote and limit neutrophil emigration.[38] High concentrations of IL-6 are found during lung inflammation,[39] and in a Cg-induced pleurisy model endogenous IL-6 was found to play a pro-inflammatory role, as reflected by reduced PML infiltration and diminished lung injury in $IL\text{-}6^{-/-}$ mice.[40] Thus, blocking these cytokines may prove to be therapeutically useful. To this end, an increase in IL-2 and IL-6 was observed in the exudates of animals following the induction of Cg-induced pleurisy compared to the NC group, and administration of compound **6P** significantly decreased these cytokines (Figure 6A and 6B).

The anti-inflammatory cytokine IL-4 plays a central role in regulating the differentiation of antigen-stimulated naive T cells into Th2 cells that produce anti-inflammatory cytokines.[41] IL-4 is also responsible for suppressing the synthesis of pro-inflammatory cytokines by macrophages and monocytes. Likewise, IL-10 is an anti-inflammatory cytokine with potent immunosuppressive

properties mediated through the downregulation of pro-inflammatory cytokines and T cell-mediated inflammatory responses.[42] During early phases of pleural inflammation, the role for IL-10 in mediating cell trafficking to the pleura and vascular leak has been indicated.[43] Furthermore, intrapleural IL-10 has been shown to inhibit the early phase of Cg-induced pleural inflammation in a murine model.[43] Thus, we wanted to assess the expression of anti-inflammatory cytokines in response to compound **6P**. To this end, we found that administration of Cg alone resulted in a significant decrease in both IL-4 and IL-10 levels compared to the NC group. Compound **6P** increased IL-4 and IL-10 cytokine levels over those seen in the Cg group, to levels significantly higher than that of even the NC group (Figure 6C and 6D).

These results demonstrate that the inflammatory process resulting from the administration of Cg into the pleural cavity caused substantially increased levels of Th1 cytokines in the pleural exudate, an effect that was diminished following treatment with compound **6P**. In contrast, compound **6P** stimulated the secretion of anti-inflammatory Th2 cytokines into the pleural exudates. Thus, these findings show that the anti-inflammatory actions of compound **6P** in this mouse model of pleurisy can be explained by a reduction in Th1 levels concurrent with an increase in Th2 cytokine release at the site of inflammation.

2.9. Effects of compound 6P on TNF-α, IL-17, and IL-10 mRNA expression in lung tissue. We studied the effect of pretreating animals with compound **6P** on the levels of TNF-α in the pleural exudates at 24 h after the induction of pleurisy by Cg and found that compound **6P** significantly inhibited the expression of TNF-α mRNA (Figure 7A). Interleukin-17 is known to play a pivotal role in the inflammatory process *via* stimulation of the synthesis of other pro-inflammatory cytokines and prostaglandins.[44] Furthermore, IL-17A is a critical mediator of neutrophil recruitment and migration. Thus, we studied the effect of pretreating animals with compound **6P**

on the expression levels of IL-17 in the lung tissue at 24 h after the induction of pleurisy by Cg injection. The Cg group exhibited a significant increase in IL-17 mRNA expression in lung tissues compared with the NC group and compound **6P** downregulated IL-17 mRNA expression (Figure 7B).

IL-10 mainly induces immunosuppressive effects through the downregulation of macrophage functions in addition to reducing monocyte/macrophage production of pro-inflammatory cytokines such as TNF-α and IL-6. Thus, IL-10 is a very important regulator of inflammation.[45] To this end, Cg-injection induces a significant decrease in IL-10 mRNA expression compared with the NC group, whereas **6P** compound treatment upregulates IL-10 expression (Figure 7C). These results indicate that compound **6P** not only induces its anti-inflammatory effect by readjusting the delicate balance among pro-inflammatory and anti-inflammatory cytokines at the level of release, but also affects this cytokine balance at the level of gene expression.

2.10. Effects of compound 6P on NF-κB p65, STAT-3, iNOS, and COX-2 mRNA expression in lung tissue. Transcription of most inflammatory mediators, including iNOS and COX-2, are controlled by NF-κB, which is kept in an inactive state in resting cells through binding to IκB.[46] Agents that inhibit NF-κB also cause decreased iNOS expression and therefore, may have beneficial therapeutic effects for the treatment of inflammatory diseases. It has previously been shown that thalidomide is capable of suppressing NF-κB activation.[47] Therefore, we performed experiments to evaluate the possible effect of compound **6P** on Cg-induced NF-κB activation. There was a significant difference in NF-κB p65 levels between NC and Cg-induced groups with the Cg-induced group exhibiting markedly increased NF-κB p65 expression. Treatment with

compound **6P** significantly inhibited NF-κB p65 activation as compared with the Cg control group (Figure 8A).

A recent study indicated that STAT-3 is both upregulated and activated in the lung following acute lung injury, and this activation is dependent on the presence of macrophages, neutrophils, and cytokines.[48] Thus, we wanted to assess if STAT-3 expression is affected by treatment with **6P**. While the Cg-treated group exhibited marked upregulation of STAT-3 expression compared with the NC group, pretreatment of mice with compound **6P** resulted in downregulation of STAT-3 mRNA expression (Figure 8B).

The activation of iNOS catalyzes the formation of a large amount of NO, which plays a key role in the pathogenesis of a variety of inflammatory diseases.[49] A significant increase in iNOS mRNA expression was detected by RT-PCR analysis in lungs of mice subjected to Cg-induced pleurisy 24 h after Cg injection. Compound **6P** treatment of mice significantly attenuated this iNOS expression (Figure 8C).

The expression of COX-2 is increased by pro-inflammatory mediators.[50] Furthermore, previous studies of two unique models of lung injury, one using IL-1β and the other TNF-α, provide convincing evidence that an increase in COX-2 gene and protein expression can be induced under inflammatory conditions.[51] Therefore, we further characterized the effects of compound **6P** treatment on Cg-induced inflammation by measuring COX-2 mRNA levels in untreated control mice, Cg-injected mice, and Cg-injected mice pre-treated with compound **6P**. These experiments showed that Cg-induced lung inflammation was associated with a significant induction in the mRNA expression of COX-2 in lung tissue, as compared to the NC group. Strikingly, pre-treatment with compound **6P** significantly reversed the changes in expression of COX-2 mRNA (Figure 8D). further supporting an anti-inflammatory role for this novel compound.

2.11. Effect of compound 6P on GITR, COX-2, STAT3, NF-κB p65, and IκBα protein expression.

We further examined the anti-inflammatory effect of compound **6P** in Cg-injected mice by measuring protein expression of inflammatory mediators. In this regard, a substantial increase in GITR protein level was observed in the lung tissue isolated from Cg-treated mice versus untreated, control mice. Acute administration of compound **6P** prior to induction of lung pleurisy by Cg resulted in a significant reduction in GITR protein (approximately 1.7 at the 20 mg/kg dose and 4.1 fold at the 40 mg/kg dose) as compared to mice in the Cg-treated group (Figure 9A). A similar trend was found for COX-2 protein expression with compound **6P** treatment diminishing COX-2 expression by approximately 2.6 and 3.7 fold over that of the Cg group (Figure 9B). Similar results were found regarding STAT-3 expression with approximately 2 and 2.8 fold reductions in activation following 6P pre-treatment of Cg-treated mice (Figure 9C). In regard to NF-κB signaling, we confirmed that nuclear translocation of the NF-κB p65 subunit is induced in mice by Cg-injection; however, pre-treatment with compound **6P** significantly inhibited this NF-κB p65 activation (approximately 2.2 and 3.8 fold) compared with the Cg group. Moreover, IκBα protein levels in lungs were substantially reduced by Cg treatment, an effect that was countered by compound **6P** (approximately 4.2 and 7.8 fold) (Figure 9D).

2.12. Histopathological examination of the effects of compound 6P.

Histological examination of lung tissues revealed that in comparison to the healthy, patent alveoli of untreated controls, lungs from Cg-injected mice showed dense inflammation with lobar lung pneumonia and thickened alveolar lung septum with occasionally obliterated alveoli (Figure 10). These sections also contain acute and inflammatory cells, interalveolar eosinophilic secretions, fibrils, and extravagated red blood cells. Pre-treatment of Cg-injected mice with compound **6P**

induced a protective effect at both doses resulting in reduced inflammation and inflammatory cell infiltration, an increase in patent areas of the lung alveoli, and overall healthier looking areas with few congestive stage patches.

2.13. Docking studies of the compound (1-10P) to the transcription factor NF-κB p65. Assuming the binding of compounds **(1-10P)** to the transcription factor NF-κB p65, the PDB structures 1MY5 and 2RAM were analyzed for potential binding sites. To determine the binding sites the software package OEDOCKING (OpenEye) was used. PDB structure 2RAM represents a novel DNA recognition mode for the NF-κB p65 homodimer. In this case the docking of test compounds into detected sites suggests an interaction of the compounds with the nucleotide residues of DNA. Results of the docking are shown in (Figure 11). In addition, the potential interaction of p65 with compounds based on the 1MY5 structures (NF-κB p65 subunit dimerization domain homodimer) and 2RAM have been considered. For this purpose, the search space of binding sites was restricted to p65 only. For the p65 from two different systems unique binding sites have been identified. Docking studies were carried out for the largest sites of each structure. Results of docking into the p65 from the 1MY5 are shown in (Figure 12), results for the site with the highest docking score for docked compounds. Involvement of the following amino acids of p65 were indicated in the interaction with the test compounds **(1-10P)**: GLU225, SER238 and ARG236. Based on chemical structure, it is likely that compounds form hydrogen bonds with ARG236 and SER238. Results of docking to p65, extracted from the complex with DNA, are shown in Figure 13. As for 1MY5, the results for the site with the highest docking score are shown. The following interactions are possible for this site and compounds: **6P** can form hydrogen bond with amino acids VAL121 and LYS123, and a hydrophobic interaction with ring of TYR36. Table 3 shows the values of docking scores for compounds **(1-10P)** that were docked into sites of the

p65 from 2RAM and 1MY5 PDB structures, respectively. Docking studies have shown the ability of this series of compounds **(1-10P)** to bind with the factor p65. Depending upon the particular complex binding can occur at different binding sites. If indeed the intended type of interaction is realized, then by the values of scoring functions the stage at which inhibition occurs may be assumed. However, the form of binding sites, namely, their location on the surface of the protein, as well as a relatively small value of the scoring function may also mean a much more complex mechanism of action of compounds in this series, not including the bonding directly with p65. Matching docking results against biological test findings allows assuming existence of correlation between the docking score and GSH level. The logarithm of the difference between activity of the particular enzyme in a disease state and its level under the test compound was chosen as a quantitative characteristic of biological activity of the test compound. Figure 14 and figure 15 shows diagrams of the docking score dependency from such a value for 1MY5 PDB-structure. Dependencies are essentially the same under all concentrations of test compound and reflect a positive correlation between absolute value of docking score and logarithmic difference. In case of 2RAM structure the correlation between these parameters is expressed to a much lesser extent. It can be explained by lack of binding to the transcription factor in a complex with DNA. Besides, based on SAR, it is not possible making any univocal conclusion on existence of relations between docking score and activity of the MDA&MPO. Presumably, other mechanisms that require further research are involved in the process. The biological activity of the compound **6P** which was selected for further study is higher than that which would be expected based on data from docking. Nevertheless, it has a fairly high docking score and generally fits the relationship previously discussed.

3. Conclusion

The results presented herein indicate that the inflammation seen in the Cg-induced pleurisy mouse model is significantly attenuated by the pre-treatment of mice with compound **6P**. Our findings suggest that this *N*-aryl phthalimide derivative may serve as a potent anti-inflammatory therapy. Further, compound **6P** (Clog *P* = 3.14) was among the most lipophilic compounds in the series due to the the insertion of the *para*-ethoxy group at the terminal phenyl ring. In fact, not only did compound **6P** significantly decrease the levels of MPO and MDA, it also increased the activity of GSH, while downregulating Th1 and upregulating Th2 cytokines in pleural exudates. Further, treatment with compound **6P** inhibits the inflammatory response, as judged by decreased T cell subsets, expression of GITR, and production of inflammatory cytokines, pro-inflammatory mediators, and NF-κB expression in lung tissue. Together, these effects result in a decrease in tissue injury.

Cumulatively, the findings presented here support the view that compound **6P** attenuates acute inflammation. Moreover, the results of this study suggest that compound **6P** possesses considerable anti-inflammatory activity, and that *N*-aryl phthalimide derivatives are a important potential source of synthetic anti-inflammatory agents.

4. Materials and methods

4.1. Biology. Heparin and λ-carrageenan (Cg) were obtained from Sigma-Aldrich (St Louis, USA). Fluoroisothiocyanate (FITC)-labeled IL-17, TNF-α and NF-κB; Phycoerythrin (PE)-labeled GITR, IL-6 and IκBα anti-mouse monoclonal antibodies; FcR blocking reagent fixation/Permeabilization and Permeabilization solutions were obtained from (Miltenyi Biotech, Germany and BD Biosciences, USA). The primers used for gene expression were purchased from Applied Biosystems (Paisley, UK) and Genscript (Piscataway, USA). High Capacity cDNA Reverse Transcription kit and SYBR® Green PCR Master Mix were purchased from Applied

Biosystems (Paisley, UK). TRIzol was purchased from Life Technologies (Grand Island, USA) Primary and secondary antibodies used for western blotting were obtained from Santa Cruz (Dallas, USA). Nitrocellulose membrane was purchased from Bio-Rad Laboratories (Hercules, USA). Chemiluminescence western blot detection kits were obtained from GE Healthcare Life Sciences (Piscataway, USA).

4.2. Animals. Female adult Balb/c mice, 6-7 weeks old and weighing 20-22 g, were obtained from the animal house of the College of Pharmacy of King Saud University, Riyadh, KSA. All the animals were acclimatized to laboratory conditions for at least one week before use in experiments. The animals were maintained under standard conditions of humidity, temperature (25 ± 2°C), and light (12-h light/12-h dark), housed in a specific pathogen-free environment and fed standard rodent chow and given water *ad libitum*. Each treatment group and vehicle control group consisted of 6 randomly-assigned animals. Animal protocol used in this study, including the use of ether as an anaesthesia agent, has been approved by the Research Ethics Committee of College of Pharmacy, King Saud University (Riyadh, Saudi Arabia). Studies reported in the manuscript fully meet the criteria for animal studies specified in the ACS ethical guidelines.

4.3. Experimental design. Induction of pleurisy by λ-carrageenan (Cg) was performed as previously described.[52] Briefly, mice were injected on the right side of the chest intrapleurally (i.pl.) with 0.1 ml normal saline (NaCl 0.9%) containing (1%) Cg. After pleurisy induction (24 h), animals were sacrificed with cervical dislocation, the chest was carefully opened, and the pleural cavity was washed with 1.0 ml of sterile phosphate buffered saline (PBS). Compounds (**1-10P**) were dispersed in normal saline with 1% of carboxymethylcellulose (CMC). For the initial screening of the novel compounds **(1-10P)**, mice were randomly divided into twelve groups (n = 6 per group). Treatments were given to each group in the following format: Group I, Normal control (NC) group animals

were injected with 0.1 ml normal saline intraperitoneally (i.p.). Group II, Cg-induced pleurisy (Cg) group, animals were injected with 0.1 mL normal saline (NaCl 0.9%) containing Cg (1%) to induce pleurisy and lung inflammation. Groups III to XII, mice received three doses of each compound **(1-10P)** (10, 20, and 40 mg/kg, i.p.) 1 h prior to Cg-induced pleurisy. Compound **6P** showed significant anti-inflammatory response and was further investigated in detail at two doses (20 and 40 mg/kg, i.p.), in the Cg-induced pleurisy mouse model. All parameters were analysed 24 after the injection of Cg.

4.4. General behaviour and acute toxicity studies in mice. The starting dose for acute oral toxicity studies of the test compounds was 2000 mg/kg. Compound number **6P** was formulated with CMC and administered by gavage. In brief, the test was performed according to OECD (1996) guidelines,[53] and after drug administration, animals were observed individually for any sign of toxicity, at least once during the first 30 min after dosing, periodically during the first 24 h (with special attention given during the first 4 h), and daily thereafter. Simultaneously, general behaviors (reactivity, gait, motor activity, ptosis, respiration, slaving, and writhing, etc.) were also observed for 7 days.

4.5. Malondialdehyde (MDA) measurement. Malondialdehyde (MDA) levels in the lung tissue were determined as an indicator of lipid peroxidation as described previously.[52] Lung tissue collected at the specified time was homogenized in 1.15% (w/v) KCl solution. A 100 µL aliquot of the homogenate was added to a reaction mixture containing 200 µL of 8.1% (w/v) SDS, 1.5 ml of 20% (v/v) acetic acid (pH 3.5), 1.5 mL of 0.8% (w/v) thiobarbituric acid and 700 µL distilled water. Samples were boiled for 1 h at 95°C using glass balls as condensers. After cooling under tap water, samples were centrifuged at 4000 x g for 10 min. and the absorbance of the supernatant was measured at 650 nm using a spectrophotometer .

4.6. Total Glutathione (GSH) Determination. Glutathione (GSH) content was estimated in lung tissue using the method of Sedlak and Lindsay[54]. The absorbance of the reaction mixture at 412 nm was read within 5 min of addition of dithibis-2-nitrobenzoic acid.

4.7. Myeloperoxidase (MPO) activity. Myeloperoxidase activity, an indicator of PML accumulation, was determined as previously described.[55] Twenty four hours following injection of carrageenan, lung tissues were obtained and weighed, and each piece was homogenized in a solution containing 05% (w/v) hexadecyltrimethyl-ammonium bromide dissolved in 10 mM potassium phosphate buffer (pH 7) and centrifuged for 30 min. at 20000 × g at 4 °C. An aliquot of the supernatant was then allowed to react with a solution of tetramethylbenzidine (1.6 mM) and 0.1 mM hydrogen peroxide. The rate of change in absorbance was measured spectrophotometrically at 650 nm. MPO activity was defined as the quantity of enzyme degrading 1 μM of peroxide/min at 37 °C and was expressed in milliunits per gram of wet tissue.

4.8. Flow cytometric analysis of $CD4^+$, $Foxp3^+$, $CD4^+Foxp3^+$, NF-κB^+, and IκB-α^+ cells in whole blood. For flow cytometric analysis of CD4, Foxp3, NF-κB, and IκB-α expression, whole blood was collected from the retro-orbital plexus (under light ether anaesthesia). Monoclonal antibody conjugated to a fluorochrome and directed against CD4 was added directly to 100 μL of whole blood, which was then lysed using a whole blood lysing reagent (BD Biosciences, USA). After centrifugation at 300 × g for 5 min., the supernatant was aspirated and 1 x fixation/permeabiliziation solution (500 μl, BD Biosciences, USA) was added to the pellet and incubated for 10 min at room temperature in the dark. The cells were then centrifuged at 300 x g for 5 min; the supernatant was aspirated and 1 x permeabilizing solution (500 μL) and FcR blocking reagent (10 μL, Miltenyi Biotech), were added to the pellet and incubated for 10 min. at room temperature in the dark. After washing with 3 mL of wash buffer, cytokine-specific antibodies (20

μL) against Foxp3, NF-κB, and IκBα (Santa Cruz and BD Biosciences, USA) were added to the cells and incubated for 30 min at room temperature in the dark. All cells were analysed for the expression of phenotypic markers on a Beckman Coulter flow cytometer (Beckman Coulter, USA) using Cytomics FC 500 software.[56] To analyse the staining of cell surface markers, the lymphocytes were first gated by their physical properties (forward and side scatter), then a second gate was drawn based on immunofluorescence characteristics of the gated cells. To determine $Foxp3^+$ the cells were gated on FSC-SSC dot plot, and then the lymphocytes were gated for analyses the percentage of $CD4^+Foxp3^+$ cells.

4.9. Flow cytometric analysis of IL-6$^+$, TNF-α$^+$, GITR$^+$ and IL-17$^+$cells in pleural exudate.

Twenty four after the injection of carrageenan, the animals were sacrificed by cervical dislocation under light ether anesthesia and the chest was carefully opened then the pleural cavity was rinsed with 1 ml saline solution containing heparin. 200 μL of this solution were pipetted directly into a 12 x 75 mm fluorescence-activated cell sorting tube containing 20 μL of a monoclonal PE-labeled IL-6 and GITR and FITC-labeled TNF-α and IL-17 antibodies (Santa Cruz and BD Biosciences, USA). The red blood cells (RBCs) were lysed by incubation in 2 mL of 1× lysis solution (BD Biosciences, USA) for 10 min. After centrifugation at 300 x g for 5 min., the supernatant was discarded, fixation/Permeabilization solution (500 μL; BD Biosciences, USA) was added to the pellet, and the samples were incubated for 10 min at room temperature in the dark. Cells were then permeabilized (500 μL, BD Biosciences, USA) and incubated for 10 min. at room temperature followed by adding, FcR blocking reagent (10 μL, Miltenyi Biotech). After washing with 3 mL of washing buffer, the antibodies specific for IL-6, TNF-α, GITR or IL-17 (20 μl; BD Biosciences, USA) were added and cells were incubated for 30 min. at room temperature in the dark. After one final wash, the stained cells were immediately analyzed by flow cytometry.[57]

4.10. Quantification of Th1 and Th2 cytokines in pleural exudate. 50 µL of the pleural exudate samples obtained from all animals, including the normal control, were collected and immediately prepared for the analysis of cytokine levels. Cytokine levels were measured with an ELISA kit according to the manufacturers' instructions (Biolegend, USA). The individual recombinant cytokines provided in the kits were used to establish standard curves.

4.11. RNA extraction and cDNA synthesis. All the extraction procedures were performed on ice using ice-cold reagents. Total RNA from the lung tissue homogenate of each mouse was isolated using the TRIzol reagent (Life Technologies, Grand Island, USA) according to the manufacturer's instructions and quantified by measuring the absorbance at 260 nm; the RNA quality was determined by measuring the 260/280 ratio. The cDNA synthesis was performed using the high-capacity cDNA reverse transcription kit (Applied Bio systems, Paisley, UK) according to the manufacturer's instructions and as previously described.[58] Briefly, 1.5 µg of total RNA from each sample was added to a mixture of 2.0 µL of 10 × reverse transcriptase buffer, 0.8 µL of 25× dNTP mix (l00 mM), 2.0 µL of l0 × reverse transcriptase random primers, 1.0 µL of multiscribe reverse transcriptase and 3.2 µL of nuclease-free water. The final reaction mixture was held at 25 °C for 10 min., then heated to 37 °C for 120 min. and 85 °C for 5 min. and, finally, cooled to 4 °C.

4.12. Real-Time Polymerase Chain Reaction (RT-PCR) determination of mRNA expression. Quantitative analysis of the mRNA expression of target genes was performed by RT-PCR by subjecting the cDNA generated from the above reaction to PCR amplification in 96-well optical reaction plates an analysis on an ABI Prism 7500 System (Applied Bio systems, Paisley, UK). The 25 µL reaction mixture included 0.1 µL of the 10 µM forward primer and 0.1 µL of the 10 µM reverse primer (each primer at a final concentration of 40 µM), 12.5 µL of the SYBR Green Universal Master mix, 11.05 µL of nuclease-free water and 1.25 µL of the cDNA sample. The primers used in the

current study (Table 2) were chosen from the PubMed database.[59] The assay controls, namely, the no-template controls, were incorporated onto the same plate to monitor the contamination of assay reagents. The RT-PCR data were analyzed using the relative gene expression (i.e., ΔΔCT) method, as described in the Applied Bio systems User Bulletin No. 2. Briefly, the data are presented as the fold change in gene expression normalized to the endogenous reference gene (GAPDH) and relative to a calibrator.

4.13. Protein extraction and western blot analysis of GITR, COX-2, STAT-3, NF-κB p65, and IκB-α. The total lung proteins were extracted from lung tissue using a previously described method.[60] Briefly, lungs were washed in ice cold PBS, cut into small pieces, and homogenized separately in cold protein lysis buffer containing a protease inhibitor cocktail.[61] Total cellular proteins were obtained by incubating the cell lysates on ice for 1 h, with intermittent vortex mixing every 10 min., followed by centrifugation at 12,000 x g for 10 min. at 4 °C. Protein concentrations were measured using the Lowry method.[62] Western blot analysis was performed using a previously described method.[63] Briefly, 25-50 µg of protein from each group was separated by 10% SDS-polyacrylamide gel electrophoresis (PAGE) and electrophoretically transferred to a nitrocellulose membrane (Bio-Rad, USA). Protein blots were blocked overnight at 4 °C, followed by incubations with primary antibodies against GITR, COX-2, STAT-3, NF-κB p65, or IκBα (Santa Cruz, Dallas, USA), followed by incubation for 2 h with peroxidase-conjugated secondary antibodies at room temperature. The GITR, COX-2, STAT-3, NF-κB p65, and IκBα bands were visualized using the enhanced chemiluminescence method (GE Health care, Mississauga, Canada) and quantified relative to β-actin bands using ImageJ®, image processing program (National Institutes of Health, Bethesda, USA). Images were taken on C-Digit chemiluminescent western blot scanner (LI-COR, Lincoln, USA).

4.14. Histopathological examination of the lung tissue. Lung tissue samples isolated from all groups were fixed for 1 week in buffered formaldehyde solution (10% in PBS) at room temperature, dehydrated using graded ethanol, and embedded in Paraplast (Sherwood Medical, Mahwah, NJ). Tissue sections (thickness 7 μm) were deparaffinised with xylene, stained with Hematoxylin and eosin (H&E) and then studied using light microscopy (Olympus, USA).

4.15. Chemistry. All the solvents were obtained from Merck. The homogeneity of the compounds was checked by TLC performed on Silica gel G coated plates (Merck). Iodine chamber was used for visualization of TLC spots. The FT-IR spectra were recorded in KBr pellets on a (Spectrum BX) Perkin Elmer FT-IR spectrophotometer. Melting points were determined on a Gallenkamp melting point apparatus, and thermometer was uncorrected. NMR Spectra were scanned in DMSO-d_6 on a Bruker NMR spectrophotometer operating at 500 MHz for ^{1}H and 125.76 MHz for ^{13}C at the Research Center, College of Pharmacy, King Saud University, Saudi Arabia. Chemical shifts δ are expressed in parts per million (ppm) relative to TMS as an internal standard and D_2O was added to confirm the exchangeable protons. Coupling constants (J) are in hertz. The following abbreviations are used in the assignment of NMR signals: s (singlet), d (doublet), m (multiplet). The compounds were purified by column chromatography on silica gel (60-120/100-200 mesh) using varied polarities of n-hexane/ethyl acetate as the eluent. The molecular masses of compounds were determined by Agilent Triple Quadrupole 6410 TQ LC/MS equipped with ESI (electrospray ionization) source. All tested compounds yielded data consistent with a purity of ≥95%, as measured by HPLC (Agilent 1260 affinity) with an ELSD (Evaporative Light Scattering Detector).

*Synthesis of 4-aminobenzohydrazide **(1)***

A mixture of (Benzocaine), ethyl 4-aminobenzoate (0.01 mol) and hydrazine hydrate (99 %, 3 mL) was refluxed for 1 h in the presence of absolute ethanol, then left to cool to room temperature. The

precipitate was filtered off, washed with water, dried and crystallized from ethanol to give **1** as white crystals.

*4-amino-N'-[substituted phenylmethylidene]benzohydrazide **(2 a-j)***

A solution of (0.01 mol) of **1** and equimolar amount of appropriate aldehyde in 60 mL of ethanol was heated under reflux for 1 h in presence of few drops of glacial acetic acid. The precipitate obtained was filtered off, washed with water and crystallized from ethanol.

*4-amino-N'-[(4-ethoxyphenyl)methylidene]benzohydrazide (**2f**):*

Yield: 70%; M.p.: 210-212 °C; IR (KBr): ν_{max}/cm^{-1}: 3420 (Ar-NH_2), 3200 (NH), 1739 (C=O); ^{1}H NMR (DMSO-d_6) δ ppm: 1.3 (3H, t, J = 7Hz, CH_3), 4.0 (2H, q, J = 9 Hz, -OCH_2), 5.7 (2H, s, -NH, D_2O exchg.), 6.5-7.6 (8H, m, Ar-H), 8.3 (1H, s, N=CH), 11.3 (1H, s, CONH, D_2O exchg.); ^{13}C NMR (DMSO-d_6) δ ppm: 15.0, 63.6, 113.0, 115.1, 120.1, 127.6, 128.8, 129.7, 146.3, 152.6, 160.2; ESI mass (*m/z*): 283.37 $[M]^+$ (calculated 283.32).

General method for the synthesis of 4-(1,3-dioxo-1,3-dihydro-2H-isoindol-2-yl)-N'-[substituted phenylmethylidene]benzohydrazide **(1-10P)**:

7.29 mmol of 4-amino-*N*'-[substituted phenylmethylidene]benzohydrazide **(2a-j)** was dissolved along with (6.75 mmol) of phthalic anhydride in 10 mL of glacial acetic acid and refluxed for 1 h. The *N*-substituted phthalimide **(1-10P)** separated out on cooling. The precipitate was filtered out through a Buchner funnel and washed twice with 30 mL of water to give the desired product. The product was recrystallized from the ethanol.

*4-(1,3-dioxo-1,3-dihydro-2H-isoindol-2-yl)-N'-[(4-nitrophenyl)methylidene]benzohydrazide **(1P)***

Yield: 80%; M.p.: 283-285 °C; IR (KBr): ν_{max}/cm^{-1}: 3258 (CONH), 2837 (N=CH), 1686 (C=O); ^{1}H NMR (DMSO-d_6) δ ppm: 7.5-8.5 (12 H, m, Ar-H), 10.8 (1H, s, N=CH), 12.2 (1H, s, CONH, D_2O exchg.); ^{13}C NMR (DMSO-d_6) δ ppm: 118.6, 119.21, 124.0, 124.5, 127.5, 127.7, 128.3, 129.1, 130.0,

131.1, 131.9, 135.3, 138.6, 141.2, 143.4, 145.2, 148.2, 163.2, 168.1, 168.2; ESI mass (*m/z*): 413.29 $[M-1]^+$ (calculated 414.37).

4-(1,3-dioxo-1,3-dihydro-2H-isoindol-2-yl)-N'-[(2-nitrophenyl)methylidene]benzohydrazide ***(2P)***

Yield: 65%; M.p.: 258-260 °C; IR (KBr): ν_{max}/cm^{-1}: 3398 (CONH), 2847 (N=CH), 1713 (C=O); ^1H NMR (DMSO-d_6) δ ppm: 7.6-8.1 (12 H, m, Ar-H), 8.9 (1H, s, N=CH), 12.1 (1H, s, CONH, D_2O exchg.); ^{13}C NMR (DMSO-d_6) δ ppm: 118.6, 124.0, 124.3, 125.1, 127.5, 127.7, 128.3, 128.4, 128.8, 129.1, 129.9, 131.0, 131.2, 131.9, 132.7, 134.1, 134.2, 135.3, 135.5, 135.9, 143.6, 148.6, 148.7, 163.2, 165.8, 167.2, 169.2; ESI mass (*m/z*): 413.86 $[M]^+$ (calculated 414.37).

N'-[(3,4-dichlorophenyl)methylidene]-4-(1,3-dioxo-1,3-dihydro-2H-isoindol-2-yl)benzohydrazide ***(3P)***

Yield: 70%; M.p.: 275-277 °C; IR (KBr): ν_{max}/cm^{-1}: 3350 (CONH), 2927 (N=CH), 1709 (C=O); ^1H NMR (DMSO-d_6) δ ppm: 7.5-8.1 (11 H, m, Ar-H), 8.3 (1H, s, N=CH), 12.2 (1H, s, CONH, D_2O exchg.); ^{13}C NMR (DMSO-d_6) δ ppm: 124.0, 124.4, 127.5, 127.7, 128.5, 128.7, 128.8, 129.8, 129.9, 131.1, 132.8, 134.3, 135.3, 135.5, 135.6, 143.2, 163.1, 167.2; ESI mass (*m/z*): 437.16 $[M-1]^+$ (calculated 438.26).

4-*(1,3-dioxo-1,3-dihydro-2H-isoindol-2-yl)-N'-[(2-methoxyphenyl)methylidene]benzohydrazide* ***(4P)***

Yield: 60%; M.p.: 253-255 °C; IR (KBr): ν_{max}/cm^{-1}: 3354 (CONH), 3065 (N=CH), 1736 (C=O); ^1H NMR (DMSO-d_6) δ ppm: 3.8 (3H, s, -OCH_3), 7.0-8.0 (12 H, m, Ar-H), 8.8 (1H, s, N=CH), 11.9 (1H, s, CONH, D_2O exchg.); ^{13}C NMR (DMSO-d_6) δ ppm: 56.1, 112.3, 121.2, 124.0, 126.0, 127.5, 127.7, 128.6, 128.8, 132.0, 135.3, 143.9, 158.2, 165.8, 167.2; ESI mass (*m/z*): 398.29 $[M-1]^+$ (calculated 399.39).

4-*(1,3-dioxo-1,3-dihydro-2H-isoindol-2-yl)-N'-[(3-hydroxyphenyl)methylidene]benzohydrazide* ***(5P)***

Yield: 58%; M.p.: 270-272 °C; IR (KBr): ν_{max}/cm^{-1}: 3352 (CONH), 2927 (N=CH), 1739 (C=O); ^1H NMR (DMSO-d_6) δ ppm: 7.1-8.0 (12 H, m, Ar-H), 8.3 (1H, s, N=CH), 9.6 (1H, s, -OH, D_2O exchg.), 11.9 (1H, s, CONH, D_2O exchg.); ^{13}C NMR (DMSO-d_6) δ ppm: 113.1, 118.0, 118.7, 119.3, 124.0, 124.3, 127.5, 128.6, 129.3, 129.9, 130.3, 132.0, 133.2, 135.2, 135.8, 136.0, 148.5, 158.1, 163.0, 167.2; ESI mass (*m/z*): 384.14 $[M-1]^+$ (calculated 385.37).

4-(1,3-dioxo-1,3-dihydro-2H-isoindol-2-yl)-N'-[(4-ethoxyphenyl)methylidene]benzohydrazide ***(6P)***

Yield: 75%; M.p.: 248-250 °C; IR (KBr): ν_{max}/cm^{-1}: 3420 (CONH), 2927 (N=CH), 1739 (C=O); ^1H NMR (DMSO-d_6) δ ppm: 1.3 (3H, t, CH_3), 4.0 (2H,q, J = 5.5 Hz, -OCH_2), 7.0-8.0 (12 H, m, Ar-H), 8.4 (1H, s, N=CH), 11.8 (1H, s, CONH, D_2O exchg.); ^{13}C NMR (DMSO-d_6) δ ppm: 15.0, 63.7, 115.2, 124.0, 127.1, 127.5, 127.7, 128.6, 128.8, 129.1, 129.2, 131.9, 135.1, 135.3, 148.4, 162.8, 167.2; ESI mass (*m/z*): 412.10 $[M-1]^+$ (calculated 413.42).

N'-[1,3-benzodioxol-5-ylmethylidene]-4-(1,3-dioxo-1,3-dihydro-2H-isoindol-2-yl)benzohydrazide ***(7P)***

Yield: 60%; M.p.: 240-242 °C; IR (KBr): ν_{max}/cm^{-1}: 3459 (CONH), 2927 (N=CH), 1739 (C=O); ^1H NMR (DMSO-d_6) δ ppm: 6.0 (2H, s, -OCH_2O-), 7.0-8.0 (12 H, m, Ar-H), 8.3 (1H, s, N=CH), 11.8 (1H, s, CONH, D_2O exchg.); ^{13}C NMR (DMSO-d_6) δ ppm: 102.0, 105.6, 108.9, 118.6, 123.9, 124.0, 124.3, 124.4, 127.5, 127.7, 128.6, 128.8, 128.9, 129.1, 129.3, 129.9, 131.9, 133.3, 135.2, 135.3, 135.8, 135.9, 148.4, 149.6, 162.9, 165.9, 167.1; ESI mass (*m/z*): 413.73 $[M]^+$ (calculated 413.38).

4-(1,3-dioxo-1,3-dihydro-2H-isoindol-2-yl)-N'-[furan-2-ylmethylidene]benzohydrazide ***(8P)***

Yield: 70%; M.p.: 283-285 °C; IR (KBr): ν_{max}/cm^{-1}: 3354 (CONH), 2926 (N=CH), 1736 (C=O); ^1H NMR (DMSO-d_6) δ ppm: 7.7-8.1 (11 H, m, Ar-H), 8.3 (1H, s, N=CH), 11.4 (1H, s, CONH, D_2O exchg.); ^{13}C NMR (DMSO-d_6) δ ppm: 124.0, 124.4, 127.7, 128.8, 129.9, 132.0, 135.3, 135.9, 165.8, 167.1; ESI mass (*m/z*): 358.20 $[M-1]^+$ (calculated 359.33).

4-(1,3-dioxo-1,3-dihydro-2H-isoindol-2-yl)-N'-[(E)-(3-nitrophenyl)methylidene]benzohydrazide ***(9P)***[64]

Yield: 60 %; M.p.: 210-212 °C; IR (KBr): ν_{max}/cm^{-1}: 3298 (CONH), 2854 (N=CH), 1712 (C=O); ^{1}H NMR (DMSO-d_6) δ ppm: 7.5-8.5 (12 H, m, Ar-H), 10.6 (1H, s, N=CH), 12.2 (1H, s, CONH, D_2O exchg.); ^{13}C NMR (DMSO-d_6) δ ppm: 119.2, 121.3, 124.6, 127.8, 128.2, 129.1, 130.0, 130.3, 130.9, 132.3, 133.8, 136.7, 139.0, 143.3, 145.3, 148.7, 163.2, 167.8, 168.3; ESI mass (*m/z*): 414. 30 $[M]^+$ (calculated 414.37).

4-(1,3-dioxo-1,3-dihydro-2H-isoindol-2-yl)-N'-[(E)-(3,4-dimethoxyphenyl)methylidene]benzohydrazide ***(10P)***[64]

Yield: 68%; M.p.: 280-282 °C; IR (KBr): ν_{max}/cm^{-1}: 3447 (CONH), 2836 (N=CH), 1740 (C=O); ^{1}H NMR (DMSO-d_6) δ ppm: 3.8 (6H, s, 2×-OCH_3), 7.0-8.0 (11 H, m, Ar-H), 8.4 (1H, s, N=CH), 11.8 (1H, s, CONH, D_2O exchg.); ^{13}C NMR (DMSO-d_6) δ ppm: 55.94, 56.0, 108.7, 111.9, 118.6, 122.4, 124.0, 124.4, 127.4, 127.5, 127.7, 128.6, 128.8, 129.9, 131.9, 133.4, 135.1, 135.3, 148.7, 149.5, 151.2, 162.9, 165.8, 167.2; ESI mass (*m/z*): 429.40 $[M]^+$ (calculated 429.42).

4.16. Docking studies of the compounds (1-10P). Structures of protein-ligand complexes were downloaded from the RCSB Protein Data Bank (PDB). Toolkit OEDOCKING3.0.1 (OpenEye) was used for docking and analysis of binding sites. Library conformer's compounds **(1-10P)** was generated by the program OMEGA2.5.1.4 (OpenEye). Detection of binding sites was performed by the program MAKE RECEPTOR3.0.1 from the toolkit OEDOCKING with "Molecular cavity detection" option. Docking compounds into these sites was performed by the program FRED with standard options.

4.17. Data analysis. All values in the figures and the text are expressed as the mean ± standard error of the mean (S.E.M.). The differences between treatment groups were analyzed by one way analysis of variance (ANOVA) followed by a Tukey-Kramer test for comparisons between groups using a computer software program (GraphPad InStat; DATASET1.ISD). A value of $*p<0.05$ was considered statistically significant.

Conflict of interest

The authors declare that there is no conflict of interest.

Acknowledgements

The authors would like to extend their sincere appreciation to the Deanship of Scientific Research at King Saud University for funding this Research Group No. (RG 1435-006).

Abbreviations Used

Cg, λ-carrageenan; NC, normal control; MDA, malondialdehyde; MPO, myeloperoxidase; GSH, glutathione; IL, interleukin; CD, cluster of differentiation; Th cells, T helper cells; ELISA, enzyme-linked immunosorbent assay; NF-κB, nuclear factor-κB; IκB-α, NF-Kappa-B inhibitor alpha; TNF-α, tumor necrosis factor-α; GITR, glucocorticoid-induced TNF receptor-related protein; Foxp3, forkhead box P3; COX-2, cyclooxygenase-2; STAT-3, signal transducer and activator of transcription-3; iNOS, inducible nitric oxide synthase; NO, nitric oxide; GM-CSF, granulocyte macrophage colony-stimulating factor; RT-PCR, reverse transcription polymerase chain reaction; mRNA, messenger RNA; PML, polymorphonuclear leukocytes, polymorphonuclear leukocyte; FITC, fluoroisothiocyanate; PE, Phycoerythrin; PBS, phosphate buffered saline; FcR, Fc Receptor blocking; RBCs; red blood cells; GAPDH, Glyceraldehyde 3-phosphate dehydrogenase; PAGE, polyacrylamide gel electrophoresis; H&E, hematoxylin and

eosin; TLC, Thin layer chromatography; HPLC, high-performance liquid chromatography; NMR, nuclear magnetic resonance; FDA, food and drug administration.

References

(1) Sampaio, E. P.; Sarno, E. N.; Galilly, R.; Cohn, Z. A.; Kaplan, G. Thalidomide selectively inhibits tumor necrosis factor alpha production by stimulated human monocytes. *J. Exp. Med.* **1991**, *173*, 699-703.

(2) Melchert, M.; List, A. The thalidomide saga. *Int. J. Biochem. Cell Biol.* **2007**, *39*, 1489-1499.

(3) Teo, S. K. Properties of thalidomide and its analogues: implications for anticancer therapy. *AAPS J.* **2005**, *7*, E1 4-9.

(4) Hashimoto, Y. Thalidomide as a multi-template for development of biologically active compounds. *Arch Pharm (Weinheim)* **2008**, *341*, 536-547.

(5) Chen, M.; Doherty, S. D.; Hsu, S. Innovative uses of thalidomide. *Dermatol. Clin.* **2010,** *28*, 577-586.

(6) Mazzon, E.; Muia, C.; Di Paola, R.; Genovese, T.; De Sarro, A.; Cuzzocrea, S. Thalidomide treatment reduces colon injury induced by experimental colitis. *Shock* **2005**, *23*, 556-564.

(7) Amirshahrokhi, K. Anti-inflammatory effect of thalidomide in paraquat-induced pulmonary injury in mice. *Int. Immunopharmacol.* **2013,** *17*, 210-215.

(8) Goli V. Does thalidomide have an analgesic effect? Current status and future directions**.** *Curr. Pain Headache Rep.* **2007**, *11*, 109-114.

(9) Rocha, A. C.; Fernandes, E. S.; Quintao, N. L. M.; Campos, M. M.; Calixto, J. B. Relevance of tumour necrosis factor-alpha for the inflammatory and nociceptive responses evoked by carrageenan in the mouse paw. *Br. J. Pharmacol.* **2006,** *148*, 688-695.

(10) Dinarello, C. A. Anti-inflammatory agents: present and future. Cell **2010**, *140*, 935-950.

(11) Niwayama, S.; Turk, B. E.; Liu, J. O. Potent inhibition of tumor necrosis factor-alpha production by tetrafluorothalidomide and tetrafluorophthalimides. *J. Med. Chem.* **1996**, *39*, 3044-3045.

(12) Muller, G. W.; Corral, L. G.; Shire, M. G.; Wang, H.; Moreira, A.; Kaplan, G. Stirling D. I., Structural modifications of thalidomide produce analogs with enhanced tumor necrosis factor inhibitory activity *J. Med. Chem.* **1996,** *39*, 3238-3240.

(13) Murai, N.; Nagai, K.; Fujisawa, H.; Hatanaka, K.; Kawamura, M.; Harada, Y. Concurrent evolution and resolution in an acute inflammatory model of rat carrageenin-induced pleurisy. *J. Leukoc. Biol.* **2003**, *73*, 456-463.

(14) Bettelli, E.; Korn, T.; Oukka, M.; Kuchroo. V. K. Induction and effector functions of T (H)17 cells. *Nature* **2008**, *453*, *1051*-1057.

(15) Mariotto, S.; Esposito, E.; Di Paola, R.; Ciampa, A.; Mazzon, E.; de Prati, A. C.; Darra, E.; Vincenzi, S.; Cucinotta, G.; Caminiti, R.; Suzuki, H.; Cuzzocrea, S. Protective effect of Arbutus unedo aqueous extract in carrageenan-induced lung inflammation in mice. *Pharmacol. Res.* **2008**, *57*, 110-124.

(16) Cuzzocrea, S.; Pisano, B.; Dugo, L.; Ianaro, A.; Maffia, P.; Patel, N. S.; Di Paola, R.; Ialenti, A.; Genovese, T.; Chatterjee, P. K.; Di Rosa, M.; Caputi, A. P.; Thiermann, C. Rosiglitazone, a ligand of the peroxisome proliferator-activated receptor-gamma, reduces acute inflammation. *Eur. J. Pharmacol.* **2004**, *483*, 79-93.

(17) Gilroy, D. W.; Newson, J.; Sawmynaden, P.; Willoughby, D. A.; Croxtall, J. D. A novel role for phospholipase A2 isoforms in the checkpoint control of acute inflammation. *FASEB J.* **2004**, *18*, 489-498.

(18) Cikla, P.; Kucukguzel, S. G.; Kucukguzel, I.; Rollas, S.; De Clercq, E.; Pannecouque, C.; Andrei, G.; Snoeck, R.; Sahin, F.; Bayrak, O. F. Synthesis and evaluation of antiviral, antitubercular and anticancer activities of some novel thioureas derived from 4-aminobenzohydrazide hydrazones. *Marmara Pharm. J.* **2010**, *14*, 13-20.

(19) Furness, B. S.; Hannaford, A. J.; Smith, P. W. G.; Tatchell, A. R. *Vogels Textbook of Practical Organic Chemistry*, 5th ed.; Longman Scientific & Technical: New York, **1991**, 1276.

(20) Kucukguzel S. G.; Mazi A.; Sahin F.; Ozturk S.; Stables J. P. Synthesis and biological activities of diflunisal hydrazide-hydrazones. *Eur. J. Med. Chem.* **2003**, *38*, 1005-1013.

(21) Pacher, P.; Beckman, J. S.; Liaudet, L. Nitric oxide and peroxynitrite in health and disease. *Physiol Rev.* **2007**, *87*, 315-424.

(22) Mullane, K. M.; Kraemer, R.; Smith, B. Myeloperoxidase activity as a quantitative assessment of neutrophil infiltration into ischemic myocardium. *J. Pharmacol. Methods* **1985**, *14*, 157-167.

(23) Kaneko, T.; Iuchi, Y.; Kobayashi, T.; Fujii, T.; Saito, H.; Kurachi, H.; Fujii, J. The expression of glutathione reductase in the male reproductive system of rats supports the enzymatic basis of glutathione function in spermato genesis. *Eur. J. Biochem.* **2002** *269*, 1570-1578.

(24) Hori, S.; Nomura, T.; Sakaguchi, S. Control of regulatory T cell development by the transcription factor Foxp3. *Science* **2003,** *299*, 1057-1061.

(25) Chung, H. S.; Park, S.; Baek, H.; Bae, H. Inhibition of LPS-induced acute lung inflammation in mice by adenovirus mediated Foxp3 expression (HYP6P.275) *J. Immunol.* **2014,** *192*, 118-120.

(26) Karin, M.; Ben-Neriah, Y. Phosphorylation meets ubiquitination: the control of NF-[kappa]B activity. *Annu. Rev. Immunol.* **2000,** *18*, 621-663.

(27) Moon, D. O.; Kim, M. O.; Kang, S. H.; Choi, Y. H.; Kim, G. Y. Sulforaphane suppresses TNF-α-mediated activation of NF-[kappa]B and induces apoptosis through activation of reactive oxygen species-dependent caspase-3. *Cancer Lett.* **2009,** *274*, 132-142.

(28) Gockel, H. R.; Lugering, A.; Heidemann, J.; Schmidt, M.; Domschke, W.; Kucharzik, T.; Lugering, N. Thalidomide induces apoptosis in human monocytes by using a cytochrome c-dependent pathway. *J. Immunol.* **2004,** *172*, 5103-5109.

(29) Rowland, T. L.; McHugh, S. M.; Deighton, J.; Dearman, R. J.; Ewan, P. W.; Kimber, I. Differential regulation by thalidomide and dexamethasone of cytokine expression in human peripheral blood mononuclear cells. *Immunopharmacology* **1998**, *40*, 11-20.

(30) Menegazzi, M.; Di Paola, R.; Mazzon, E.; Genovese, T.; Crisafulli, C.; Dal Bosco, M.; Zou, Z.; Suzuki, H.; Cuzzocrea, S. Glycyrrhizin attenuates the development of carrageenan-induced lung injury in mice. *Pharmacol. Res.* **2008**, *58*, 22-31.

(31) Stow, J. L.; Low, P. C.; Offenhauser, C.; Sangermani, D. Cytokine secretion in macrophages and other cells: pathways and mediators. *Immunobiology* **2009**, *214*, 601-612.

(32) Nocentini, G.; Riccardi, C. GITR: a multifaceted regulator of immunity belonging to the tumor necrosis factor receptor superfamily. *Eur. J. Immunol.* **2005**, *35*, 1016-1022.

(33) Cuzzocrea, S.; Ronchetti, S.; Genovese, T.; Mazzon, E.; Agostini, M.; Di Paola, R.; Esposito, E.; Muia, C.; Nocentini, G.; Riccardi, C. Genetic and pharmacological inhibition of GITR-GITRL interaction reduces chronic lung injury induced by bleomycin instillation. *FASEB J.* **2007,** *21*, 117-129.

(34) Li, L.; Huang, L.; Vergis, AL.; Ye, H.; Bajwa, A.; Narayan, V.; Strieter, R. M.; Rosin, D. L.; Okusa, M.D. IL-17 produced by neutrophils regulates IFN-gamma-mediated neutrophil migration in mouse kidney ischemia-reperfusion injury. *J. Clin. Invest.* **2010**, *120*, 331-342.

(35) Dinarello, C. A. Proinflammatory Cytokines. *Chest*. **2000**, *118*, 503-508.

(36) Sinkovics, J. G.; Horvath, J. C. Human natural killer cells: a comprehensive review. *Int. J. Oncol.* **2005**, *27*, 5-47.

(37) De sanctis, J. B., Blanca, I., Bianco, N. E. Secretion of cytokines by natural killer cells primed with interleukin-2 and stimulated with different lipoproteins. *Immunology*. **1997**, *90*, 526-533.

(38) Rijneveld, A. W.; van den Dobbelsteen, G. P.; Florquin, S.; Standiford, T. J.; Speelman, P.; van Alphen, L.; van der Poll, T. Roles of interleukin-6 and macrophage inflammatory protein-2 in pneumolysin-induced lung inflammation in mice. *J. Infect. Dis.* **2002**, *185*, 123-126.

(39) Jin, J.; Zeng, H.; Schmid, K. W.; Toetsch, M.; Uhlig, S.;, Moroy, T. The zinc finger protein Gfi1 acts upstream of TNF to attenuate endotoxin-mediated inflammatory responses in the lung. *Eur. J. Immunol.* **2006,** *36*, 421-430.

(40) Cuzzocrea, S.; Sautebin, L.; De Sarro, G.; Costantino, G.; Rombola, L.; Mazzon, E.; Ialenti, A.; De Sarro, A.; Ciliberto, G.; Di Rosa, M.; Caputi, A. P.; Thiemermann, C. Role of IL-6 in the pleurisy and lung injury caused by carrageenan. *J. Immunol.* **1999**, *163*, 5094-5104.

(41) Seder, R. A.; Paul, W. E.; Davis, M. M.; Fazekas de. St. Groth, B. The presence of interleukin 4 during in vitro priming determines the lymphokine-producing potential of CD4C T cells from T cell receptor transgenic mice. *J. Exp. Med.* **1992**, *176*, 1091-1098.

(42) Cuzzocrea, S.; Mazzon, E.; Calabro, G.; Dugo, L.; De Sarro, A.; van De Loo, F. A.; Caputi, A. P. Inducible nitric oxide synthase-knockout mice exhibit resistance to pleurisy and lung injury caused by carrageenan. *Am. J. Respir. Crit. Care Med.* **2000**, *162*, 1859-1866.

(43) Oberholzer, A.; Oberholzer, C.; Moldawer, L. L. Interleukin-10: a complex role in the pathogenesis of sepsis syndromes and its potential as an anti-inflammatory drug. *Crit. Care Med.* **2002**, *30*, S58-S63.

(44) Hurst, S. D.; Muchamuel, T.; Gorman, D. M.; Gilbert, J. M.; Clifford, T.; Kwan, S. New IL-17 family members promote Th1 or Th2 responses in the lung: in vivo function of the novel cytokine IL-25. *J. Immunol.* **2002**, *169*, 443-453.

(45) De Kozak, Y.; Thillaye-Goldenberg, B.; Naud, M. C.; Da Costa, A. V.; Auriault, C.; Verwaerde, C. Inhibition of experimental autoimmune uveoretinitis by systemic and subconjunctival adenovirus-mediated transfer of the viral IL-10 gene. *Clin. Exp. Immunol.* **2002**, *130*, 212-223.

(46) Di Marco, B.; Massetti, M; Bruscoli S; Macchiarulo, A; Di Virgilio, R.; Velardi, E.; Donato, V.; Migliorati, G.; Riccardi, C. Glucocorticoid-induced leucine zipper (GILZ)/NF-kappaBinteraction: role of GILZ homo-dimerization and C-terminal domain. *Nucleic Acids Res.* **2007,** *35*, 517-528.

(47) Majumdar, S.; Lamothe, B.; Aggarwal, B. B. Thalidomide suppresses NF-kB activation induced by TNF and H2O2, but not that activated by ceramide, lipopolysaccharides, or phorbol ester. *J. Immunol.* **2002,** *168*, 2644-2651.

(48) Gao, H.; Guo, R. F.; Speyer, C. L.; Reuben, J.; Neff, T. A.; Hoesel, L. M. Stat3 activationin acute lung injury. *J. Immunol.* **2004,** *172*, 7703-7712.

(49) Korhonen, R.; Lahti, A.; Kankaanranta, H.; Moilanen, E. Nitric oxideproduction and signaling in inflammation. *Curr. Drug Targets Inflamm. Allergy* **2005**, *4*, 471-179.

(50) Kim, H. J.; Kim, K. W.; Yu, B. P.; Chung, H. Y. The effect of age on cyclooxygenase-2 gene expression: NF-kappaB activation and IkappaBalpha degradation. *Free Radic. Biol. Med.* **2000**, *28*, 683-692.

(51) Gust, R.; Kozlowski, J. K.; Stephenson, A. H.; Schuster, D. P. Role of cyclooxygenase-2 in oleic acid-induced acute lung injury. *Am. J. Respir. Crit. Care Med.* **1999,** *160*, 1165-1170.

(52) Cuzzocrea, S.; Mazzon, E.; Dugo, L.; Serraino, I.; Ciccolo, A.; Centorrino, T.; De Sarro, A.; Caputi, A. P. Protective effects of n-acetylcysteine on lung injury and red blood cell modification induced by carrageenan in the rat. ***FASEB J.*** **2001**, *15*, 1187-2000.

(53) Guidelines for testing of Chemicals. Organization for economic cooperation and development guideline 423, acute oral toxicity-acute toxic class method. *OECD Guideline* **2001,** 1-14.

(54) Sedlak, J.; Lindsay, R. H. Estimation of total, protein-bound, and nonprotein sulfhydryl groups in tissue with Ellman's reagent. *Anal. Biochem.* **1968,** *25*, 192-205.

(55) Laight, D. W.; Lad, N.; Woodward B, Waterfall JF. Assessment of myeloperossidase activity in renal tissue after ischemia-reperfusion. *Eur. J. Pharmacol.* **1994**, *292*, 81-88.

(56) Ahmad, S. F.; Zoheir, K. M.; Bakheet, S. A.; Ashour, A. E.; Attia, S. M. Poly(ADP-ribose) polymerase-1 inhibitor modulates T regulatory and IL-17 cells in the prevention of adjuvant induced arthritis in mice model. *Cytokine* **2014,** *68*, 76-85.

(57) Ahmad, S. F.; Zoheir, K. M.; Ansari, M. A.; Korashy, H. M.; Bakheet, S. A.; Ashour, A. E.; Al-Shabanah, O. A.; Al-harbi, M. M.; Attia, S. M. The role of poly(ADP-ribose) polymerase-1 inhibitor in carrageenan-induced lung inflammation in mice. *Mol. Immunol.* **2015,** *63*, 394-405.

(58) Ahmad, S. F.; Zoheir, K. M.; Abdel-Hamied, H. E.; Alrashidi, I.; Attia, S. M.; Bakheet, S. A.; Ashour, A. E.; Abd-Allah, A. R. The role of a histamine 4 receptor as an anti-inflammatory target in carrageenan-induced pleurisy in mice. *Immunology* **2014**, *142*, 374-383.

(59) Ahmad, S. F.; Attia, S. M.; Bakheet, S. A.; Zoheir, K. M.; Ansari, M. A.; Korashy, H. M.; Abdel-Hamied, H. E.; Ashour, A.; Abd-Allah, A. R. Naringin attenuates the development of carrageenan-induced acute lung inflammation through inhibition of NF-κb, STAT3 and pro-inflammatory mediators and enhancement of IκBα and anti-inflammatory cytokines. *Inflammation*. **2015**, *38*, 846-857.

(60) Barakat, A.; Szick-Miranda, K.; Chang, I. F.; Guyot, R.; Blanc, G.; Cooke, R.; Delseny, M.; Bailey-Serres, J. The organization of cytoplasmic ribosomal protein genesin the Arabidopsis genome. *Plant Physiol.* **2001**, *127*, 398-415.

(61) Ansari, M. A.; Maayah, Z. H.; Bakheet, S. A.; El-Kadi, A. O.; Korashy, H. M. The role of aryl hydrocarbon receptor signaling pathway in cardiotoxicity of acute lead intoxication in vivo and in vitro rat model. *Toxicology* **2013**, *306*, 40-49.

(62) Seevaratnam, R.; Patel, B. P.; Hamadeh, M. J. Comparison of total protein con-centration in skeletal muscle as measured by the Bradford and Lowry assays. *J. Biochem.* **2009**, *145*, 791-797.

(63) Green, M. R.; Sambrook, J. Molecular Cloning. A Laboratory Manual, 4th Ed.; Cold Spring Harbour Laboratory Press: Plain view, New York, 2012.

(64) Bhat, M. A.; Al-Omar, M. A. Synthesis, characterization and invivo anticonvulsant and neurotoxicity screening of Schiff bases of phthalimides. *Acta Pol. Pharm.* **2011**, *68*, 375-380.

Table 1. Effect of compounds **(1-10P)** on MDA levels, MPO and GSH activity in the lung tissue at 24 h after the induction of pleurisy by Cg injection.

Groups	Dose (mg/kg)	MDA level (µM /mg protein)	GSH activity (µM /mg protein)	MPO activity (µM/mg protein)
Normal (NC)	-	65.14 ± 5.48	10.08 ± 0.61	35.33 ± 3.62
Carrageenan (Cg)	-	214.59 ± 13.50**	6.87 ± 0.64**	88.34 ± 5.81**
1P	**10**	191.54 ± 10.86	7.12 ± 0.60	71.66 ± 5.77
	20	185.27 ± 11.74	7.59 ± 0.76	70.23 ± 5.35
	40	154.68 ± 11.94[a]	8.94 ± 0.66[a]	68.04 ± 5.37[a]
2P	**10**	188.68 ± 10.79	7.01 ± 0.44	67.96 ± 5.62
	20	182.58 ± 13.91	7.2 ± 0.42	65.11 ± 4.38[a]
	40	173.03 ± 12.14	7.54 ± 0.44	55.58 ± 5.22[a]
3P	**10**	180.18 ± 11.92	6.9 ± 0.76	64.85 ± 4.04
	20	175.56 ± 10.21	8.56 ± 0.64[a]	60.84 ± 4.99
	40	141.48 ± 8.81[a]	7.23 ± 0.59	51.37 ± 5.48[a]
4P	**10**	181.18 ± 8.92	6.27 ± 0.86	72.85 ± 5.04
	20	163.56 ± 12.54	7.08 ± 0.74	67.84 ± 5.99
	40	151.48 ± 13.81[a]	7.2 ± 0.99	62.37 ± 6.48[a]
5P	**10**	166.12 ± 10.24	7.43 ± 0.72	70.16 ± 5.30
	20	151.50 ± 12.73[a]	7.62 ± 0.64	68.45 ± 5.50
	40	132.66 ± 11.49[a]	8.05 ± 0.73	62.81 ± 5.23[a]
6P	**10**	80.24 ± 11.25[a]	9.06 ± 0.7[a]	50.45 ± 5.27[b]
	20	71.74 ± 9.42[b]	9.3 ± 0.90[b]	42.66 ± 4.11[b]
	40	68.32 ± 10.16[b]	9.51 ± 0.71[b]	39.26 ± 4.86[b]
7P	**10**	178.45 ± 9.41	7.02 ± 0.66	59.66 ± 5.82
	20	170.97 ± 7.92	7.4 ± 0.82	52.36 ± 3.52[a]
	40	132.51 ± 7.58[a]	7.83 ± 0.67[a]	77.85 ± 5.60
8P	**10**	169.49 ± 8.71	8.70 ± 0.92[a]	72.07 ± 5.05
	20	176.26 ± 12.76	7.65 ± 0.39[a]	79.68 ± 6.51
	40	165.07 ± 13.55	7.99 ± 0.63[a]	76.99 ± 5.26
9P	**10**	183.15 ± 13.53	6.99 ± 0.71	71.49 ± 3.65
	20	177.03 ± 12.75	7.9 ± 0.83[a]	66.1 ± 3.37
	40	155.91 ± 11.29[a]	8.1 ± 0.69[b]	50.41 ± 5.53[b]
10P	**10**	191.38 ±11.67	7.01 ± 0.75	79.12 ± 5.20
	20	180.92 ± 10.83	7.65 ± 0.69	74.91 ± 5.65
	40	160.34 ± 11.26[b]	8.01 ± 0.83[a]	65.35 ± 5.09[a]

Statistical analysis was performed using a one-way ANOVA followed by the Tukey-Kramer post-test. Each value indicates the mean ± S.E.M of six animals. $^{*}P<0.05$ and $^{**}P<0.01$ compared to the normal control (NC) group; $^{a}P<0.05$ and $^{b}P<0.01$ compared to Carrageenan control (Cg) group.

Table 2. Primers sequence. TNF-α, Tumor necrosis factor-alpha; IL, Interleukin; NF-κB, Nuclear Factor-KappaB; STAT-3, Signal transducer and activator of transcription-3; iNOS, Inducible nitric oxide synthase; COX-2, Cyclooxygenase-2; GAPDH, Glyceraldehyde 3-phosphate dehydrogenase.

Targeted gene	Direction and Sequence
TNF-α	F: 5'-GCGGAGTCCGGGCAGGTCTA-3' R: 5'-GGGGGCTGGCTCTGTGAGGA-3'
IL-17	F: 5'-ATCCCTCAAAGCTCAGCGTGTC-3'R: 5'-GGGTCTTCATTGCGGTGGAGAG-3'
IL-10	F: 5'-ACCTGCTCCACTGCCTTGCT-3' R: 5'-GGTTGCCAAGCCTTATCGGA-3'
NF-κB p65	F: 5'- ACACCTCTGCATATAGCGGC-3' R: 5'- GGTACCCCCAGAGACCTCAT-3'
STAT-3	F: 5'-CCCCCGTACCTGAAGACCAAG-3'; R: 5'-TCCTCACATGGGGGAGGTAG-3'
iNOS	F: 5'-CTATGGCCGCTTTGATGTGC-3'; R: 5'-CAACCTTGGTGTTGAAGGCG-3'
COX-2	F: 5'-CACTCATGAGCAGTCCCCTC-3'; R: 5'-ACCCTGGTCGGTTTGATGTT-3'
GAPDH	F: 5'-CCCAGCAAGGACACTGAGCAAG-3'R: 5'-GGTCTGGGATGGAAATTGTGAGGG-3'

Table 3: Docking scores for compounds **(1-10P)** into sites of the p65 from 1MY5 PDB and 2RAM structures.

	FRED Chemgauss4 score for 3-series	
	1MY5	2RAM
1P	-2.95667	-2.04628
2P	-2.87152	-3.70965
3P	-2.75688	-2.39803
4P	-2.59486	-3.34522
5P	-3.12665	-3.8724
6P	-2.93576	-2.34406
7P	-2.5249	-2.2963
8P	-3.23412	-3.51448
9P	-1.77481	-1.94317
10P	-2.65739	-1.86046

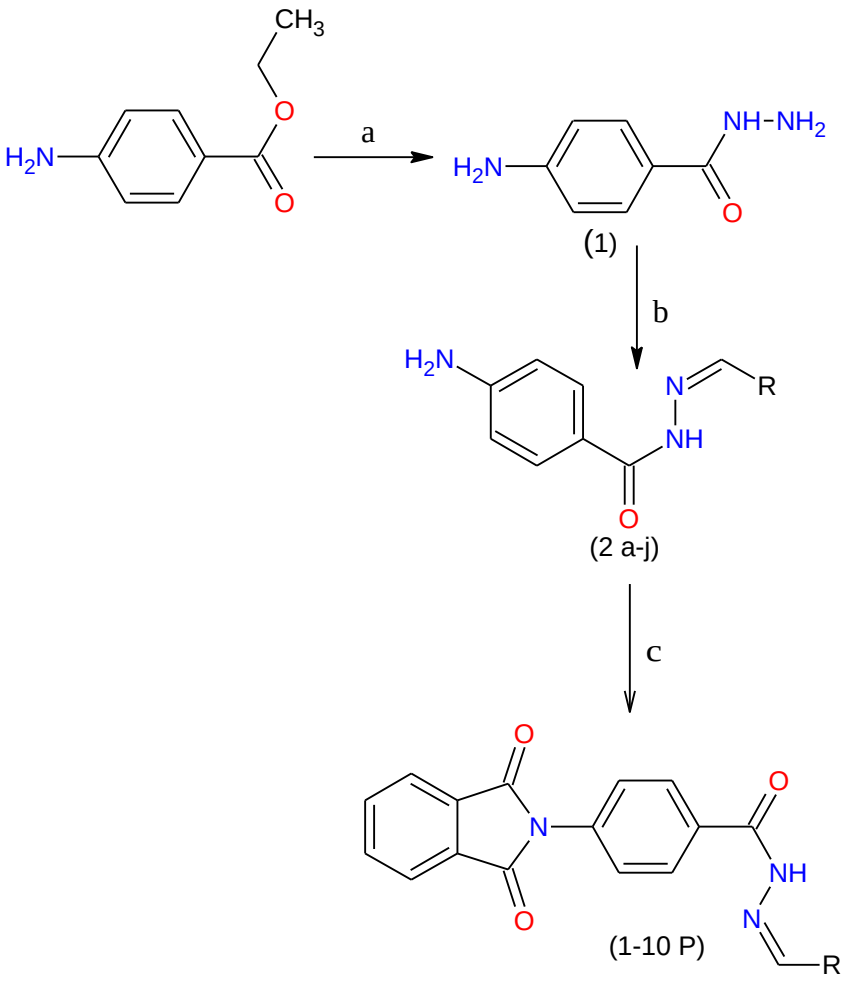

Compound	R
1P	4-Nitrophenyl
2P	2-Nitrophenyl
3P	2,4-Dichlorophenyl
4P	2-Methoxyphenyl
5P	3-Hydroxyphenyl
6P	4-Ethoxyphenyl
7P	Piperonal
8P	Furfural
9P	3-Nitrophenyl
10P	3,4-Dimethoxyphenyl

Scheme 1. Synthetic route of compounds **(1-10P)**.(a) NH_2-NH_2.H_2O/Absolute EtOH, reflux; (b) RCHO/EtOH, AcOH, reflux 1 h; (c) Phthalic anhydride, AcOH, reflux 1 h.

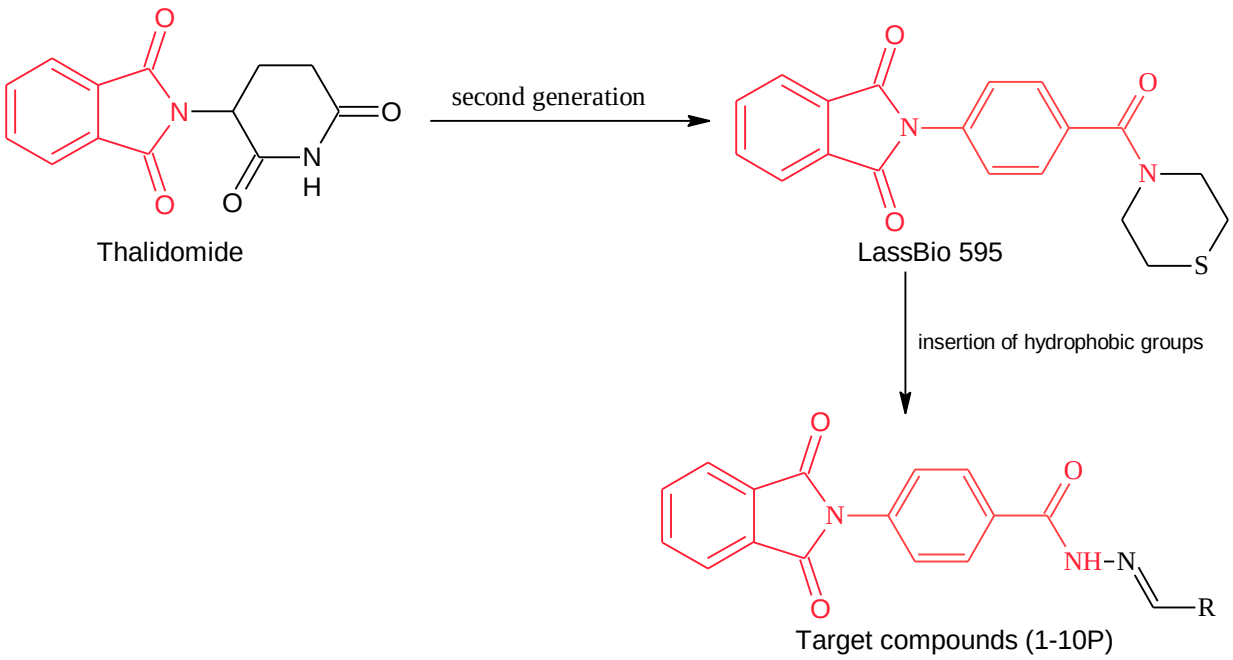

Figure 1. Design of the *N*-aryl phthalimide derivatives **(1-10P)**.

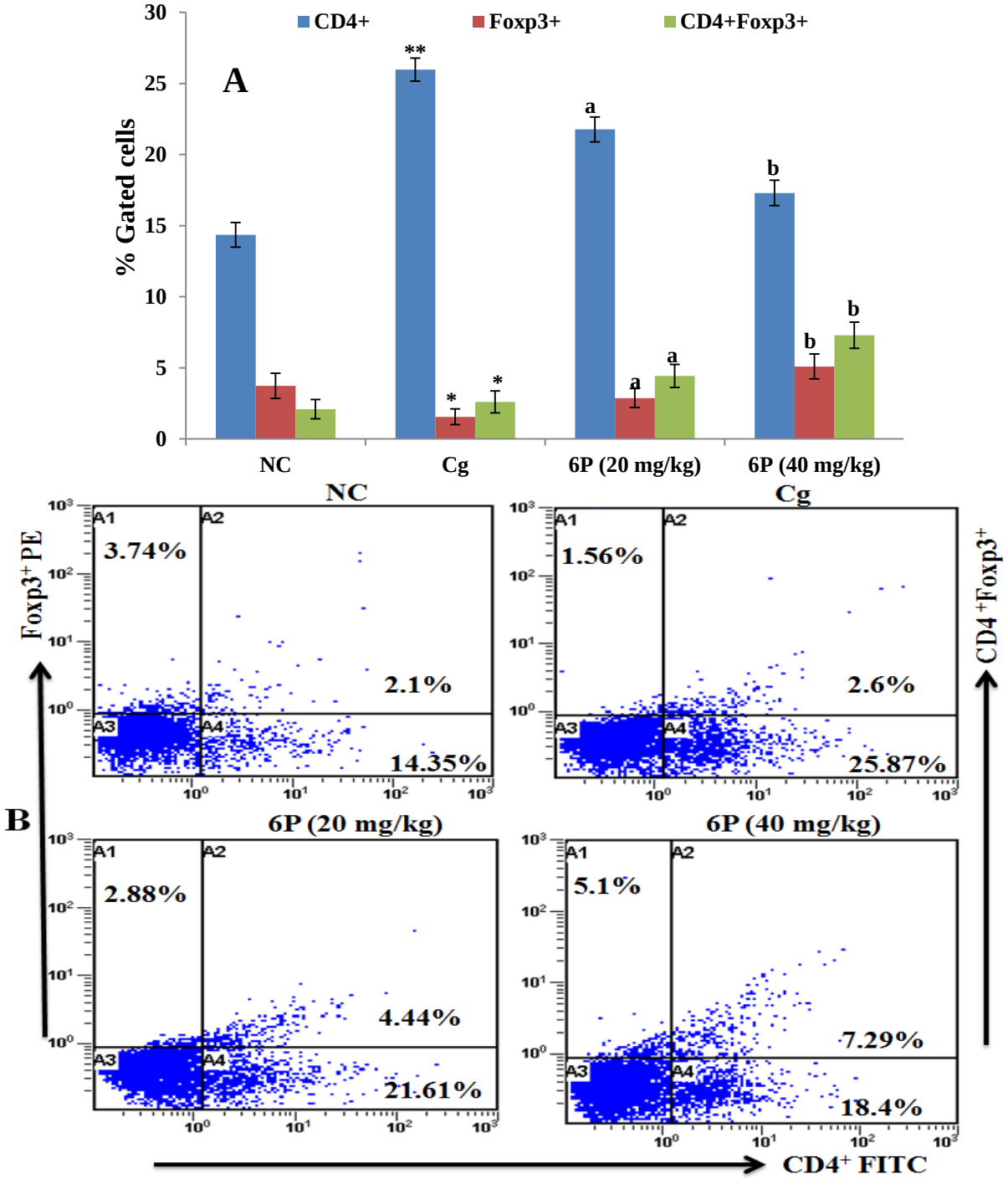

Figure 2 A. Effect of compound **6P** on $CD4^+$, $Foxp3^+$, and $CD4^+Foxp3^+$ populations. Flow cytometric analysis of $CD4^+$, $Foxp3^+$ and $CD4^+Foxp3^+$ expression in whole blood at 24 h after the induction of pleurisy via Cg injection. B. Representative dot plots are shown for $CD4^+$, $Foxp3^+$, and $CD4^+Foxp3^+$ expressing cells in the whole blood from one mouse from each group at 24 h. Statistical analysis was performed using a one-way ANOVA followed by the Tukey-Kramer post-test. Each value indicates the mean ± S.E.M of six animals. $^*P<0.05$ and $^{**}P<0.01$ compared to the normal control (NC) group; $^aP<0.05$ and $^bP<0.01$ compared to Carrageenan control (Cg) group.

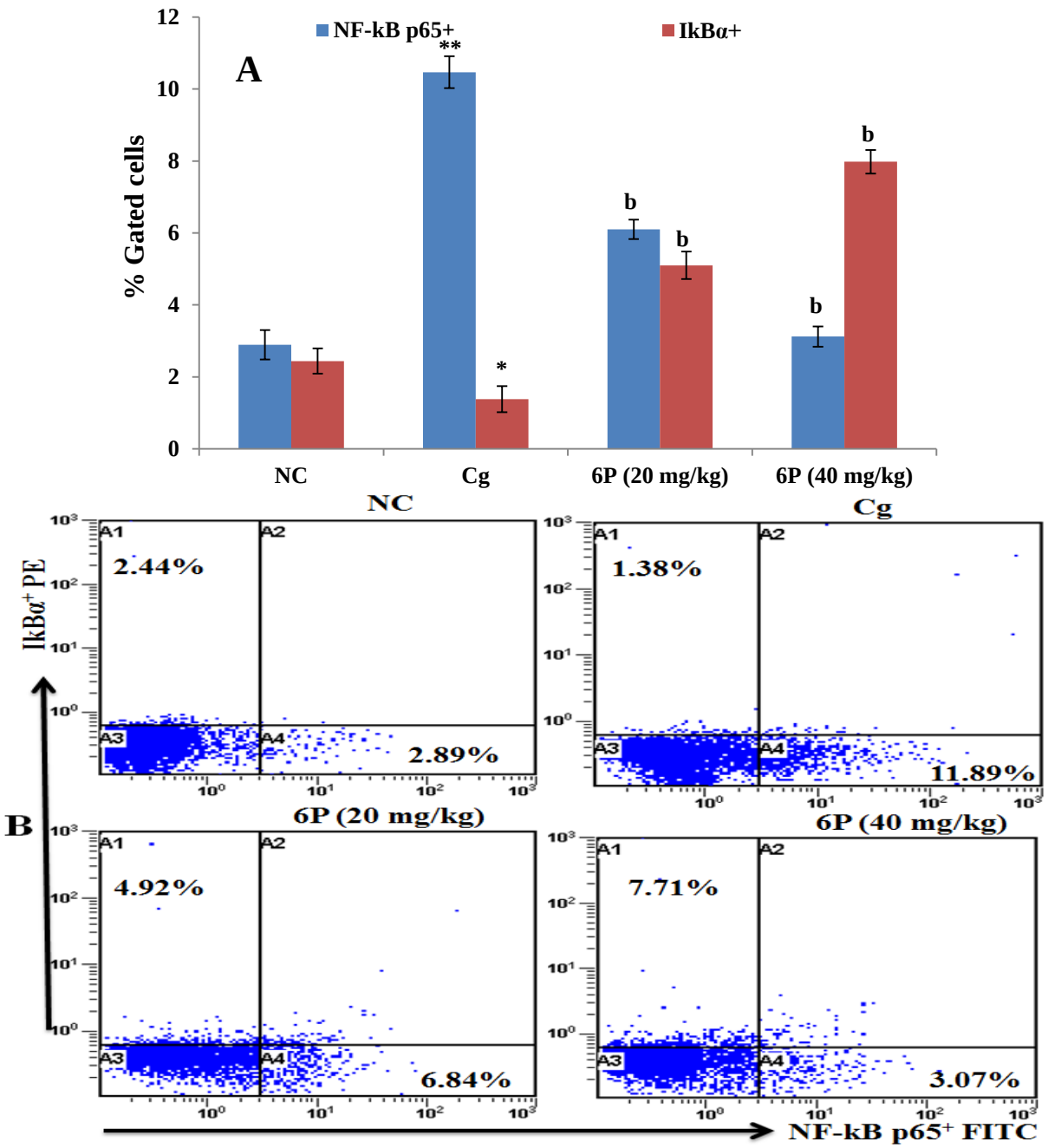

Figure 3 A. Effect of compound **6P** on NF-κB p65$^+$, and IκBα$^+$ populations. Flow cytometric analysis of NF-κB p65$^+$, and IκBα$^+$ expression on cells in whole blood at 24 h after the induction of pleurisy via Cg injection. B. Representative dot plots are shown for NF-κB p65$^+$, and IκBα$^+$ expressing cells in the whole blood from one mouse from each group at 24 h. Statistical analysis was performed using a one-way ANOVA followed by the Tukey-Kramer post-test. Each value indicates the mean ± S.E.M of six animals. $^*P<0.05$ and $^{**}P<0.01$ compared to the normal control (NC) group; $^aP<0.05$ and $^bP<0.01$ compared to Carrageenan control (Cg) group.

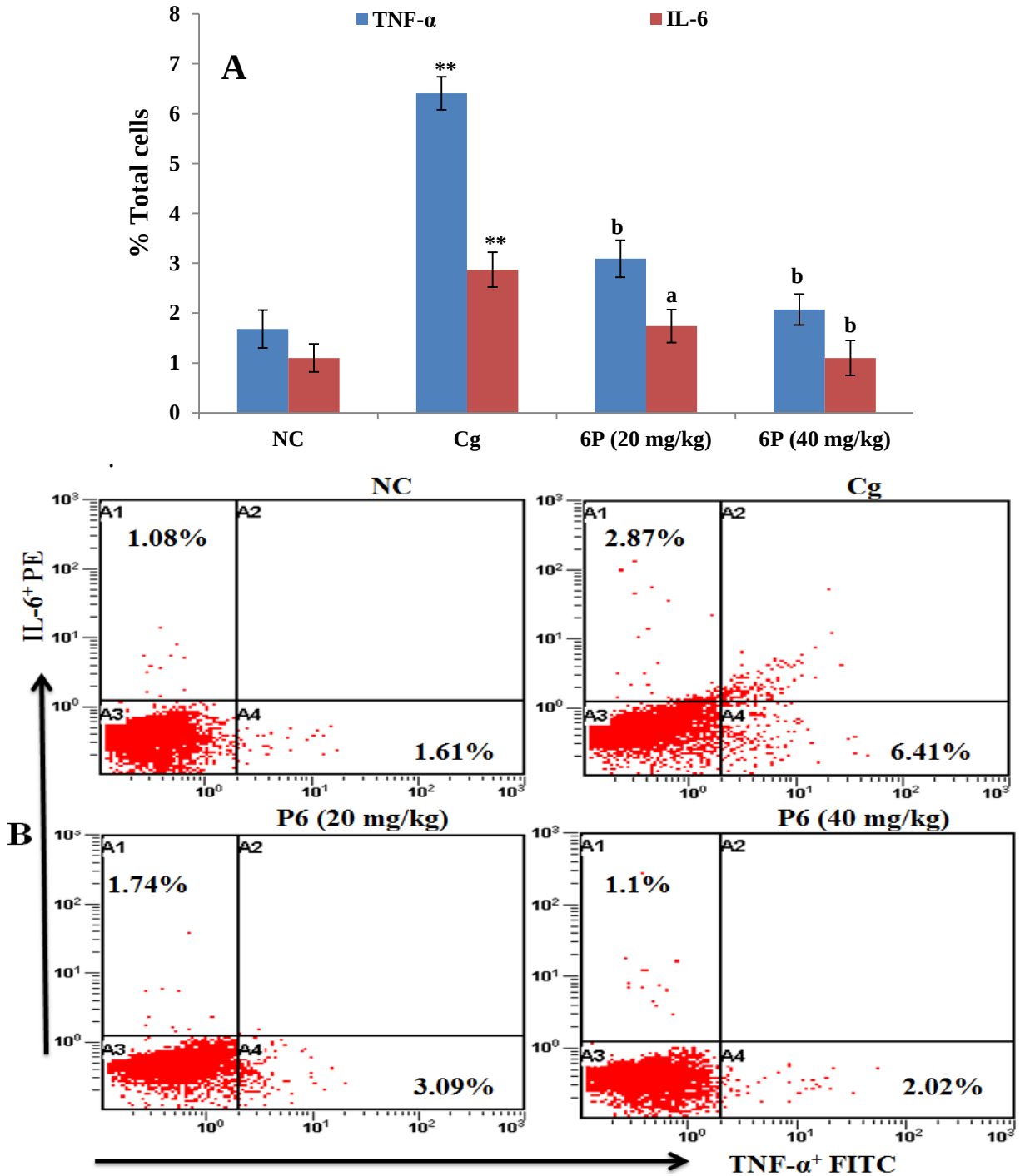

Figure 4 A. Effect of compound **6P** on TNF-α$^+$ and IL-6$^+$ populations in pleural exudate. Flow cytometric analysis of TNF-α$^+$ and IL-6$^+$ expression on pleural exudate cells at 24 h after the induction of pleurisy *via* Cg injection. **B.** Representative dot plots are shown for TNF-α and IL-6 expressing cells in the whole blood from one mouse from each group at 24 h. Statistical analysis was performed using a one-way ANOVA followed by the Tukey-Kramer post-test. Each value indicates the mean ± S.E.M of six animals. $^{*}P<0.05$ and $^{**}P<0.01$ compared to the normal control (NC) group; $^{a}P<0.05$ and $^{b}P<0.01$ compared to Carrageenan control (Cg) group.

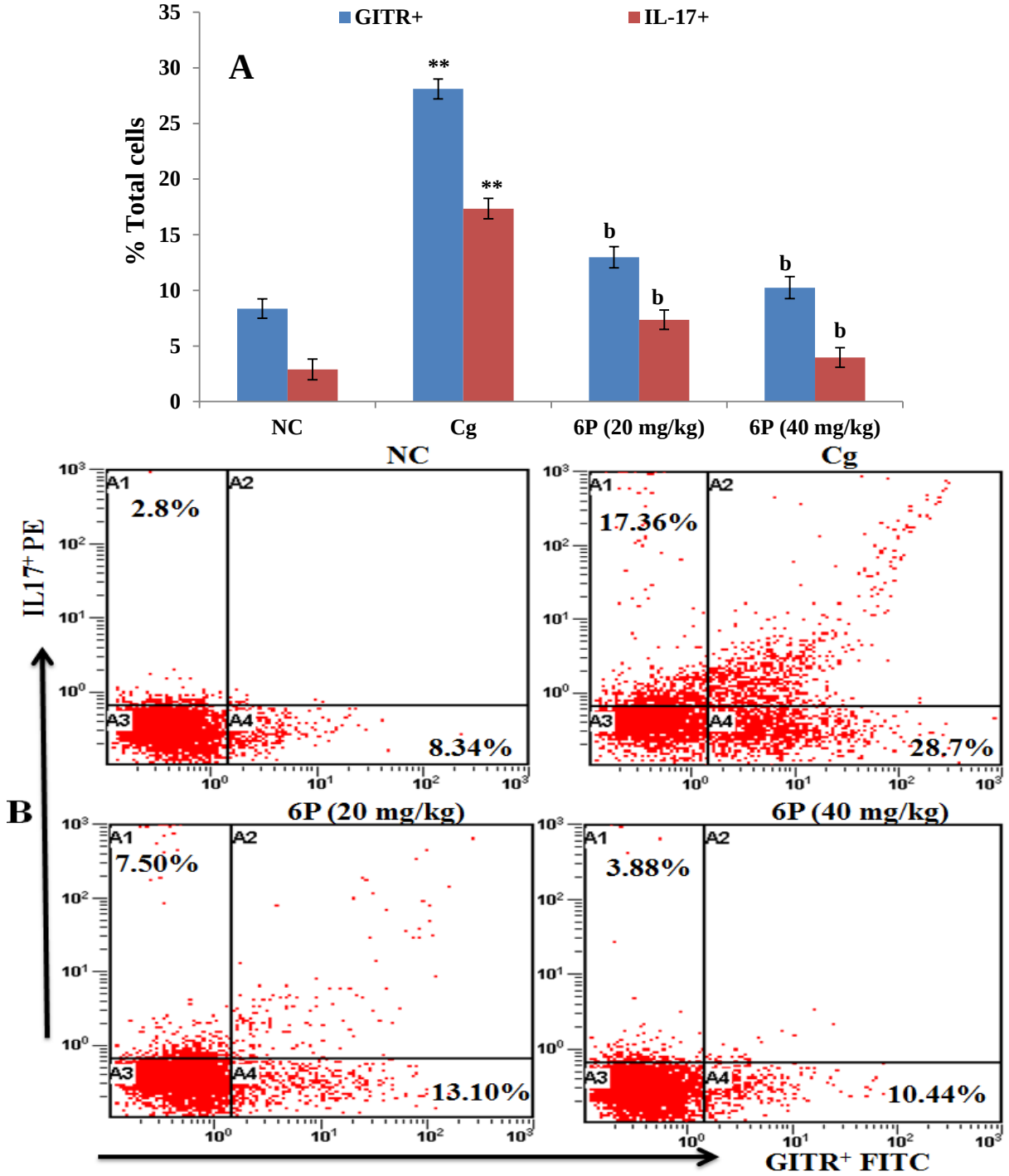

Figure 5 A. Effect of compound **6P** pretreatment on GITR$^+$ and IL-17$^+$ populations in pleural exudate. Flow cytometric analysis of GITR and IL-17 expression on pleural exudate cells at 24 h after the induction of pleurisy *via* Cg injection. **B.** Representative dot plots are shown for GITR and IL-17 expressing cells in the whole blood from one mouse from each group at 24 h. Statistical analysis was performed using a one-way ANOVA followed by the Tukey-Kramer post-test. Each value indicates the mean ± S.E.M of six animals. $^{*}P<0.05$ and $^{**}P<0.01$ compared to the normal control (NC) group; $^{a}P<0.05$ and $^{b}P<0.01$ compared to Carrageenan control (Cg) group.

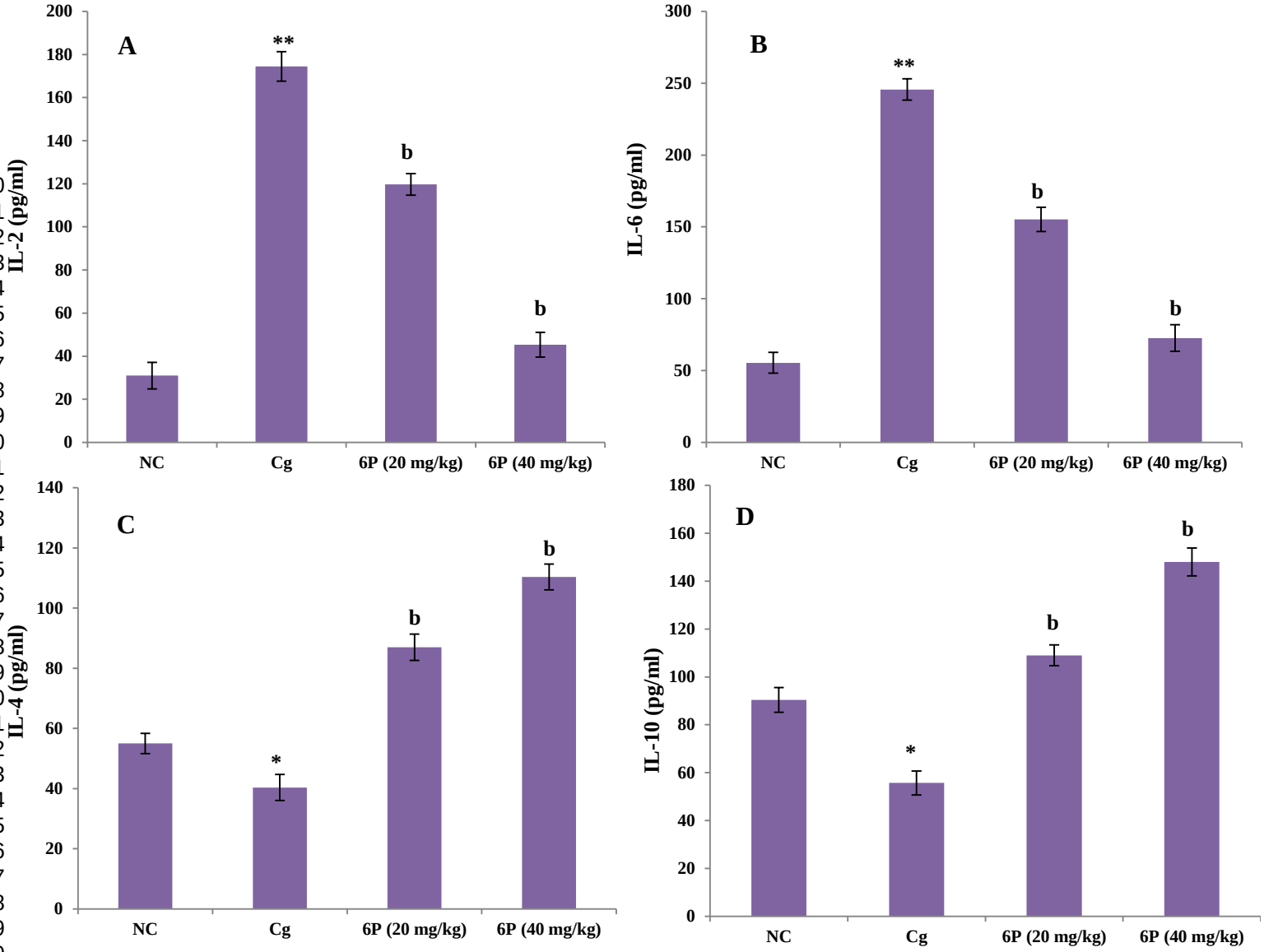

Figure 6. Effect of compound **6P** on the levels of IL-2 **(A)**, IL-6 **(B),** IL-4 **(C)** and IL-10 **(D).** The levels of pro- and anti-inflammatory cytokines were evaluated by ELISA from the exudates at 24 after the induction of pleurisy by Cg injection. Statistical analysis was performed using a one-way ANOVA followed by the Tukey-Kramer post-test. Each value indicates the mean ± S.E.M of six animals. $^{*}P<0.05$ and $^{**}P<0.01$ compared to the normal control (NC) group; $^{a}P<0.05$ and $^{b}P<0.01$ compared to Carrageenan control (Cg) group.

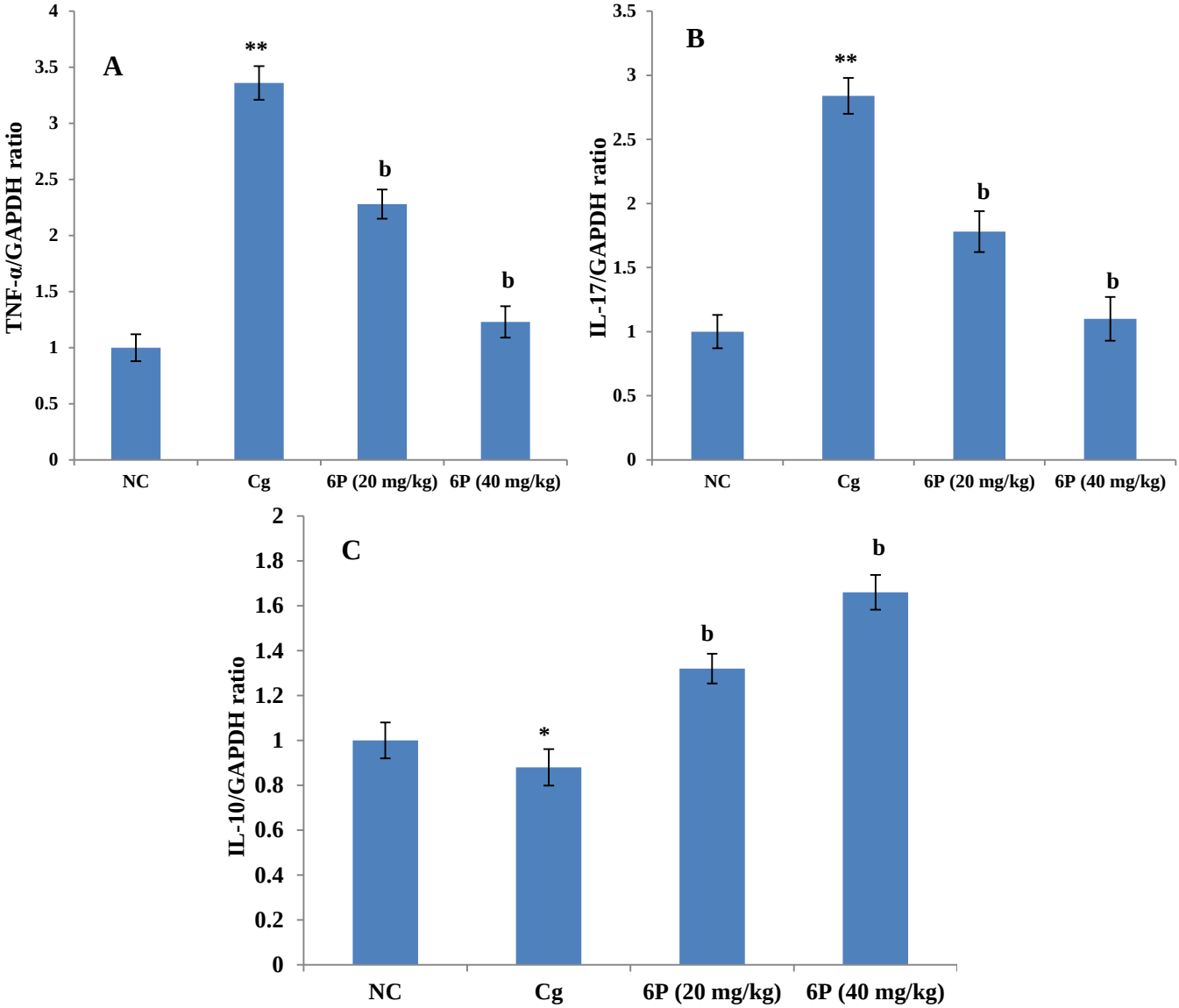

Figure 7. Effect of compound **6P** on the gene expression of pro- and anti-inflammatory **(A)** TNF-α, **(B)** IL-17 and **(C)** IL-10 cytokines. mRNA expression was measured by quantitative RT-PCR in the lung tissue at 24 h after the induction of pleurisy by Cg injection. Statistical analysis was performed using a one-way ANOVA followed by the Tukey-Kramer post-test. Each value indicates the mean ± S.E.M of six animals. $^{*}P<0.05$ and $^{**}P<0.01$ compared to the normal control (NC) group; $^{a}P<0.05$ and $^{b}P<0.01$ compared to Carrageenan control (Cg) group.

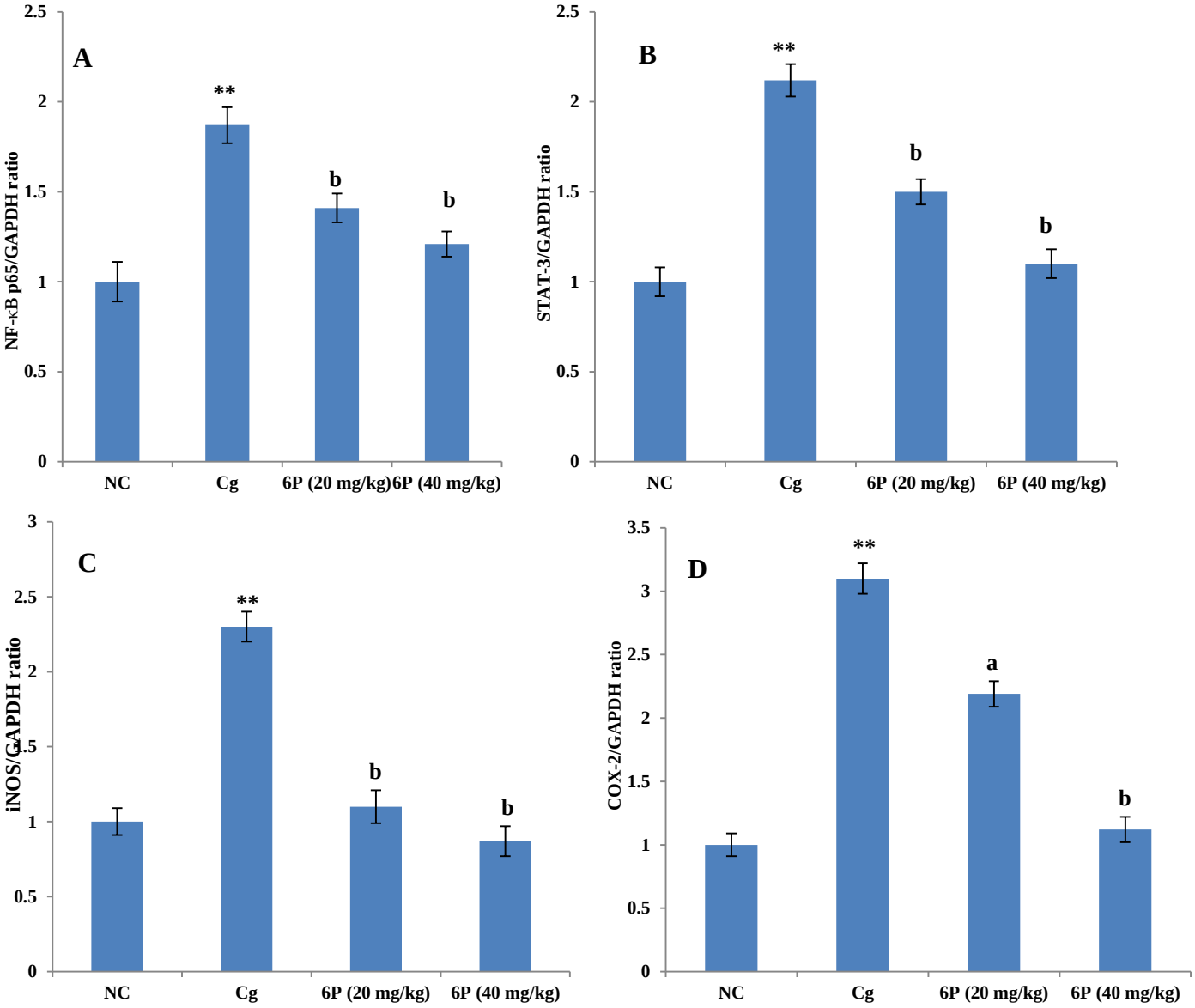

Figure 8. Effect of compound **6P** on the gene expression of **(A)** NF-κB P65, **(B)** STAT-3, **(C)** iNOS and **(D)** COX-2. mRNA expression was measured by quantitative RT-PCR in the lung tissue at 24 h after the induction of pleurisy by Cg injection. Statistical analysis was performed using a one-way ANOVA followed by the Tukey-Kramer post-test. Each value indicates the mean ± S.E.M of six animals. $^{*}P<0.05$ and $^{**}P<0.01$ compared to the normal control (NC) group; $^{a}P<0.05$ and $^{b}P<0.01$ compared to Carrageenan control (Cg) group.

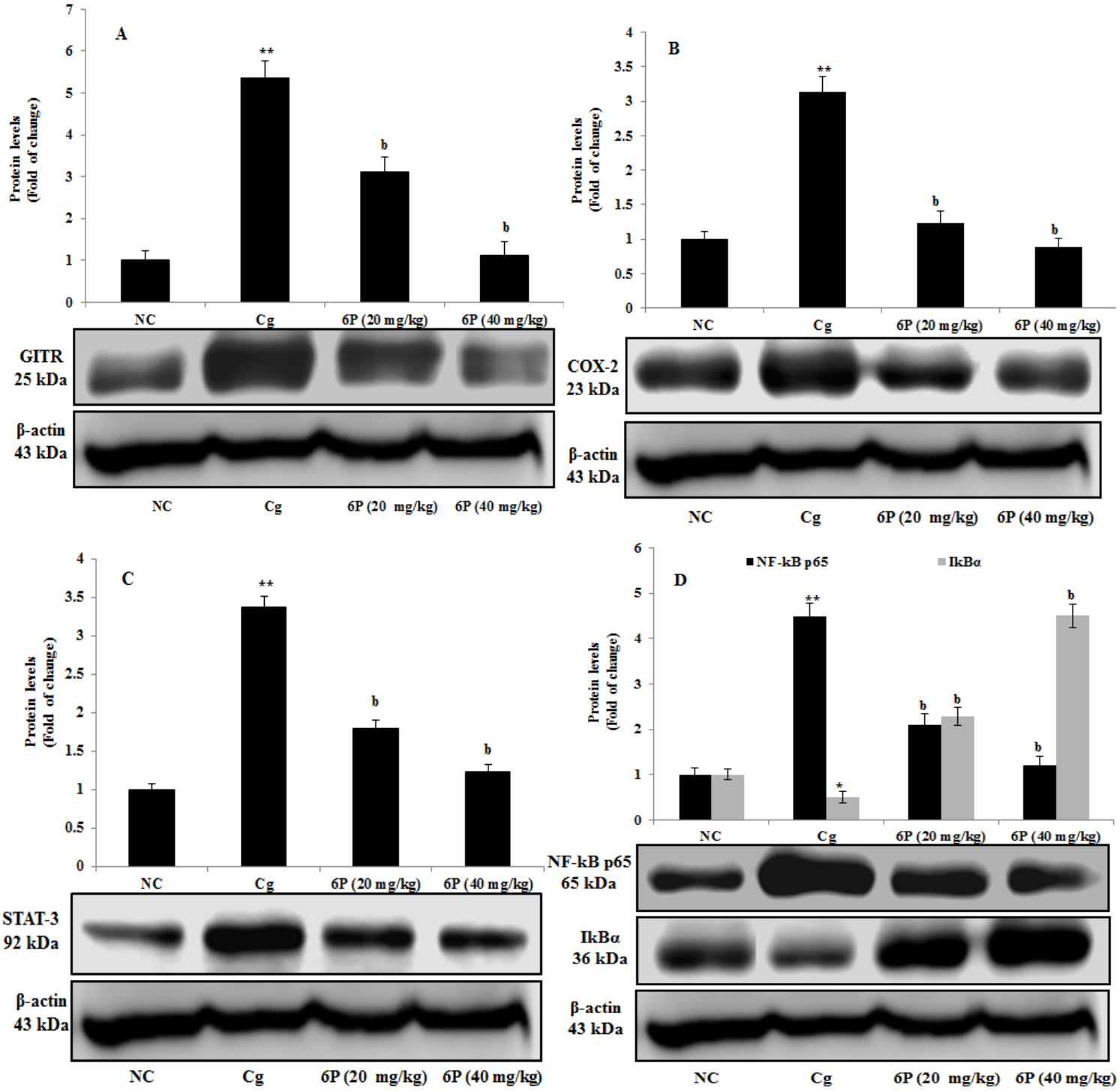

Figure 9. Effect of compound **6P** on the protein levels of **(A)** GITR, **(B)** COX-2, **(C) STAT-3** and **(D)** NF-κB p65. Statistical analysis was performed using a one-way ANOVA followed by the Tukey-Kramer post-test. Each value indicates the mean ± S.E.M of six animals. $^{*}P<0.05$ and $^{**}P<0.01$ compared to the normal control (NC) group; $^{a}P<0.05$ and $^{b}P<0.01$ compared to Carrageenan control (Cg) group.

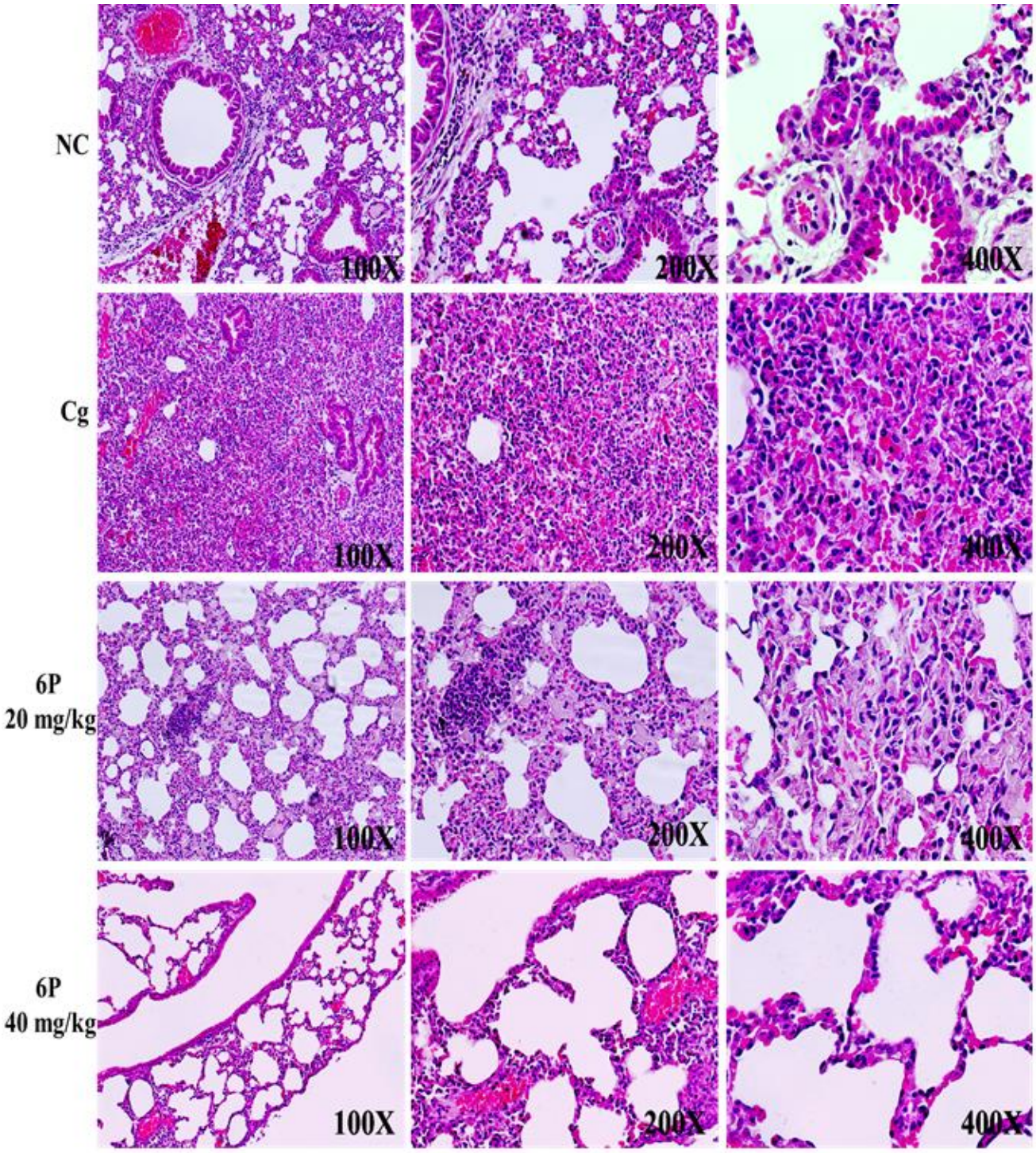

Figure 10. Histopathological examinations of lung tissue stained with haematoxylin and eosin under a light microscope (100, 200, and 400 X). Animals were treated with compound **6P** (20 or 40 mg/kg, i.p.), and histopathologically examined at 24 h after Cg injection.

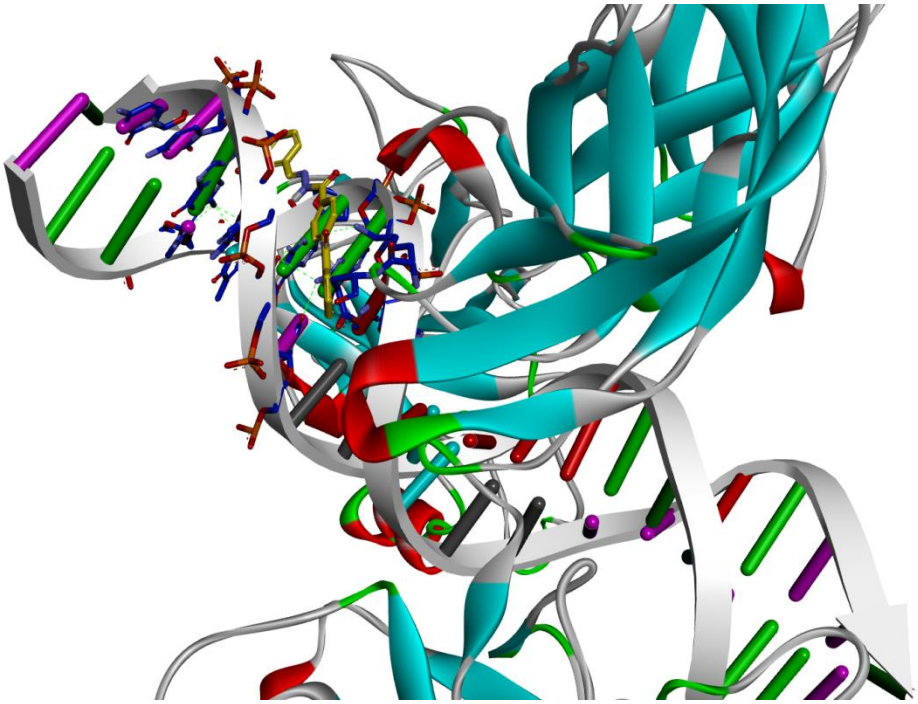

Figure 11. Binding of compound **6P** with complex NF-κB p65 with DNA

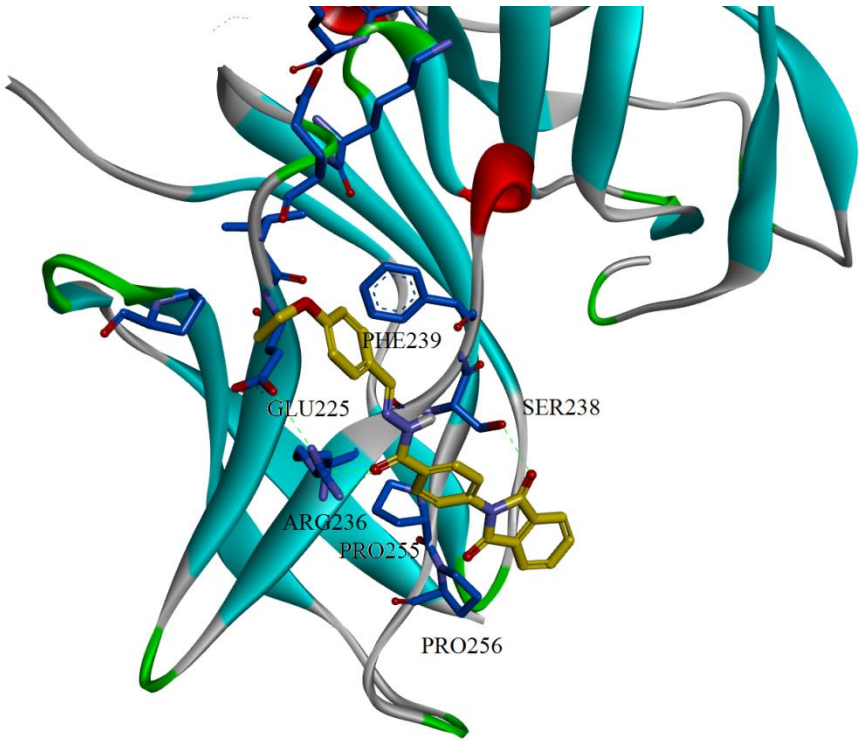

Figure 12. Results of docking of the compound **6P** into detected binding site for 1MY5.

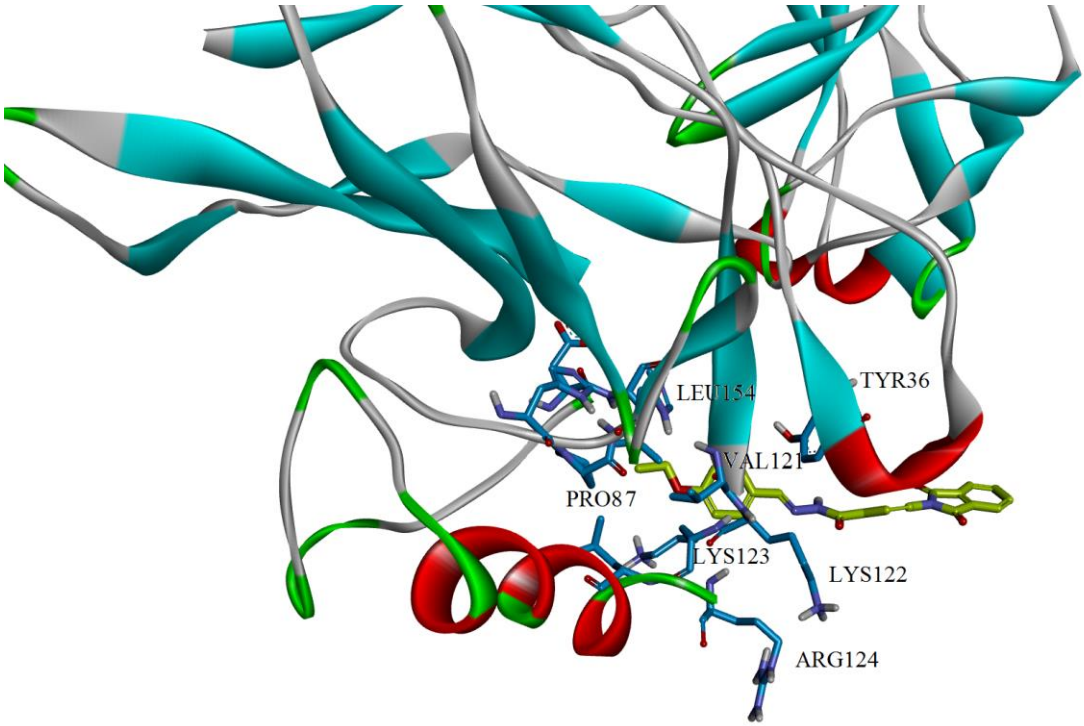

Figure 13. Compound **6P** in binding site of 2RAM.

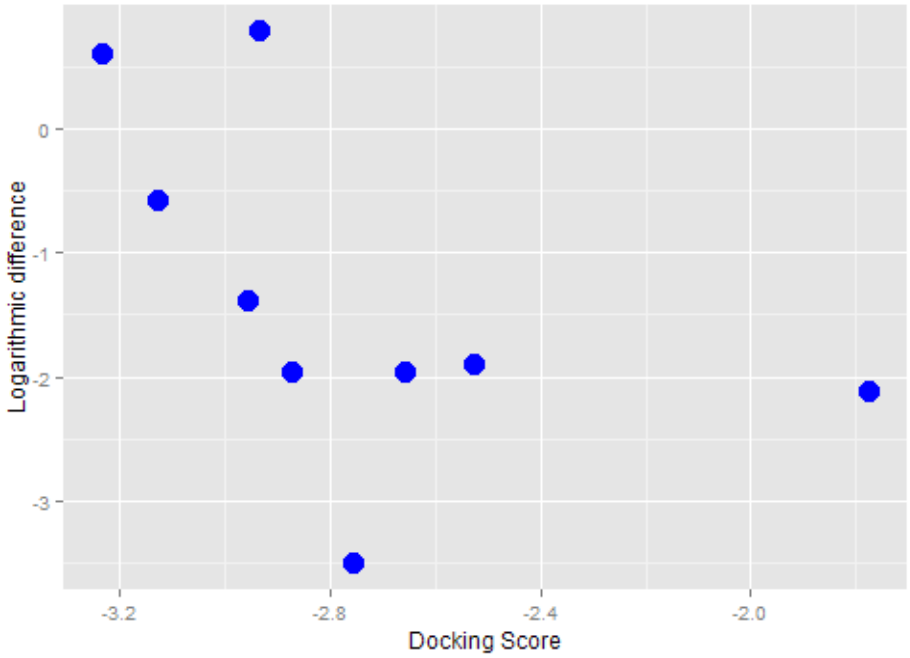

Figure 14*: Correlation between the docking score for 1MY5 pdb-structure and GSH level (10 mg/Kg).

*number of points in the figures 14 and 15 differ due to the measured value for the activity of the GSH protein in the case with compound 4P. GSH activity for this compound are below the disease level, so the difference has a negative value.

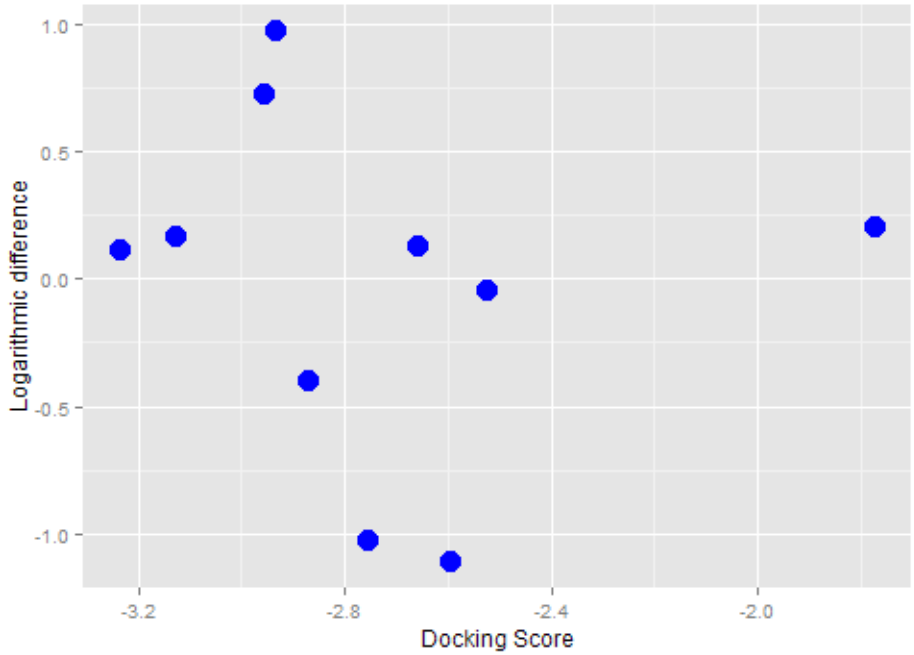

Figure 15: Correlation between the docking score for 1MY5 pdb-structure and GSH level (40 mg/Kg).